The Krishnaswamy Laboratory

Yale Genetics and Yale SEAS present

Machine Learning

for

Single Cell Analysis

Online - May 20-29, 2020

What is your favorite model organism?

Machine Learning for Single Cell Analysis

Course introduction

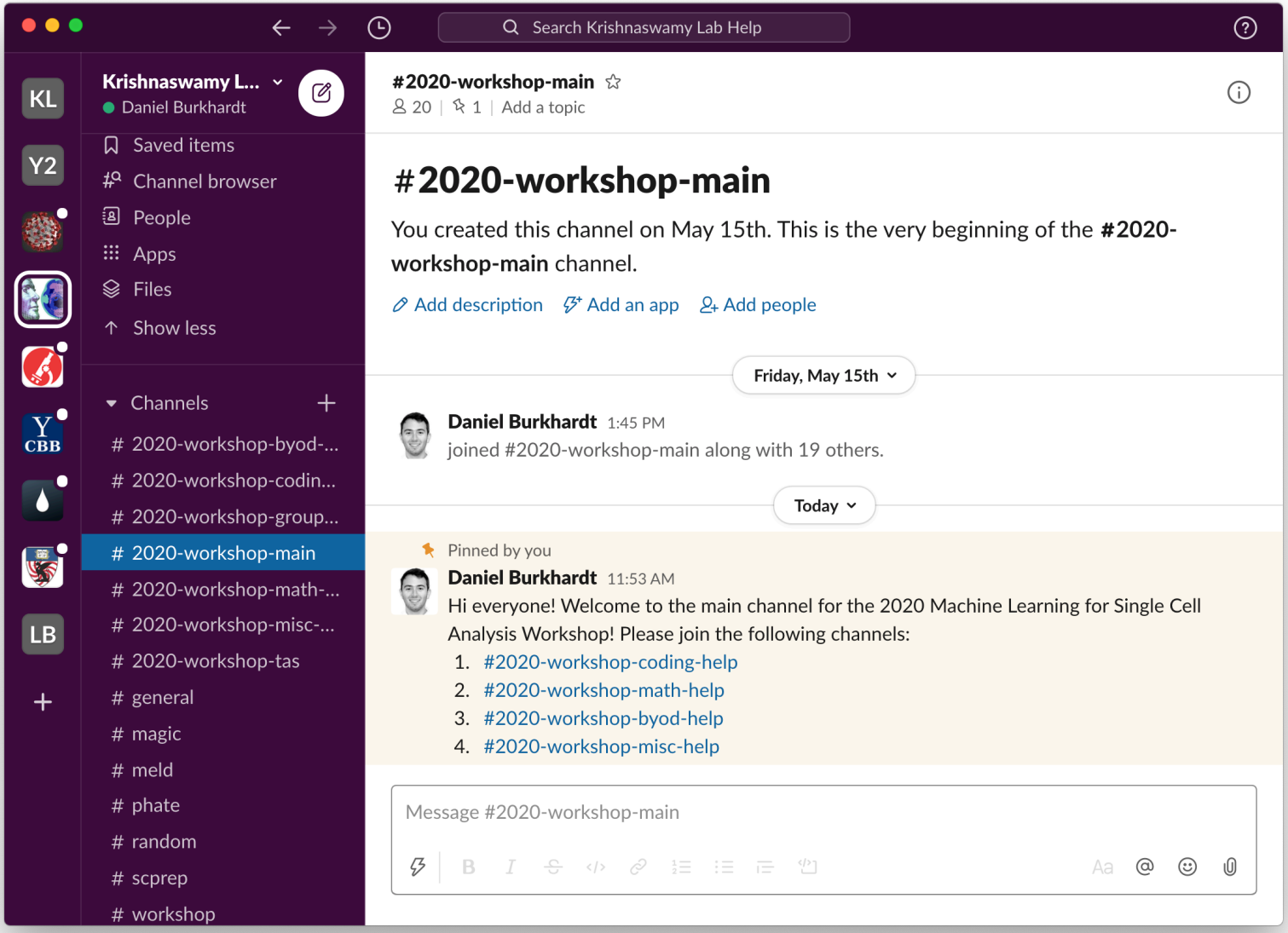

https://krishnaswamylab.org/get-help


UMass Amherst
Mount Sinai
City of Hope
Irell and Manella Graduate School of Biological Sciences
Johns Hopkins University
McMaster University
University of Copenhagen
מכון ויצמן למדע
Weizmann Institute of Science
Institute for Systems Biology
Whitehead Institute
Columbia University in the City of New York
Northeastern University
Washington University in St. Louis
UCL
Yale
Georgia Tech
University of Cambridge
University of Virginia
University of Washington
McGill
UCLA
Universitas Indonesia
Faculty of Medicine
St. Jude Children's Research Hospital
Finding cures. Saving children.
Junta de Andalucía
Fundación Progreso y Salud
Consejería de Salud
Institut Pasteur
novo nordisk
University of Zurich[UZH]
CSH
Cold Spring Harbor Laboratory
Harvard University
IGIB
Institute of Genomics & Integrative Biology
Genomics Knowledge Partner

Big biomedical data

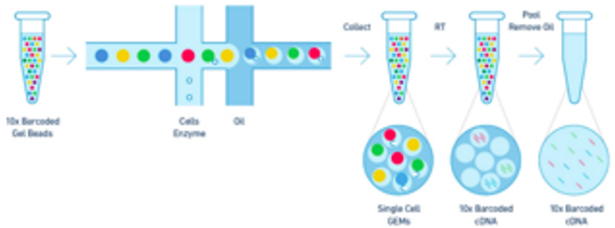

ScRNA-seq

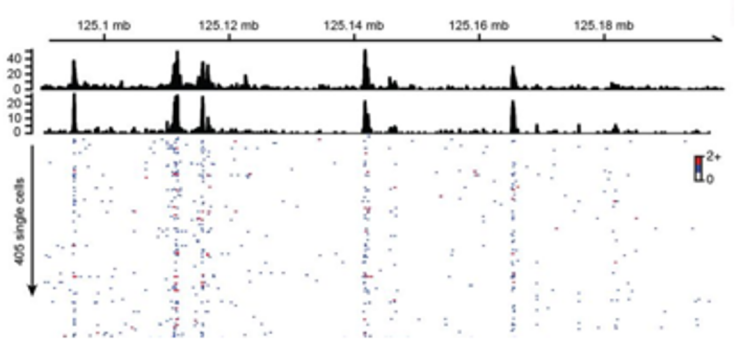

ScATAC-seq

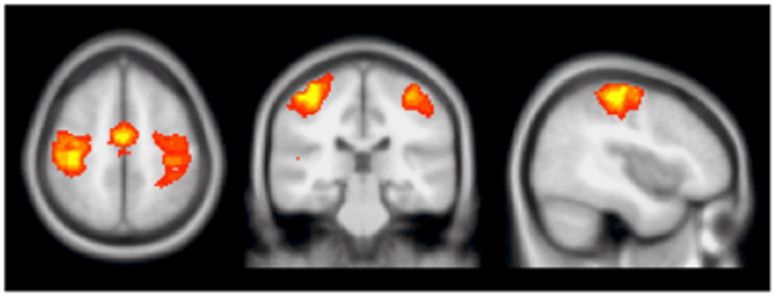

FMRI

Patient Data

Big = Any dataset with many many observations

The single cell revolution

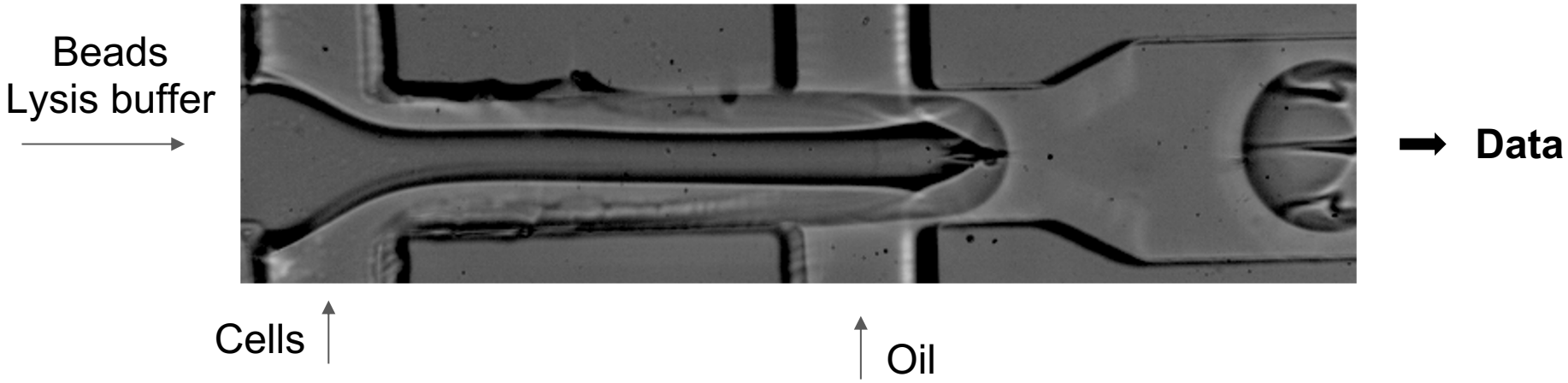

The single cell revolution

Interesting Biological Experiments

Computation

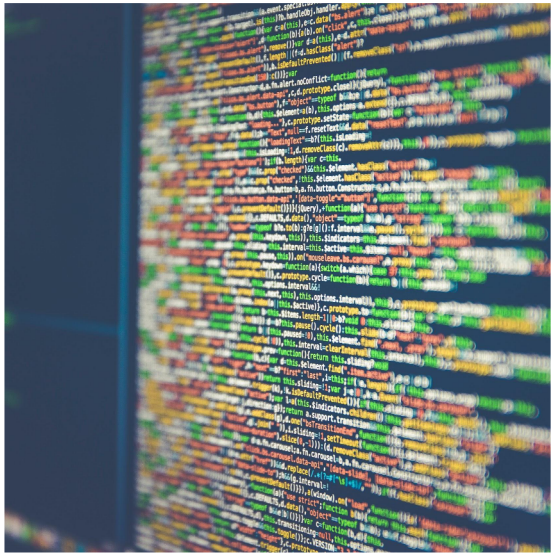

High impact paper

LETTER

https://doi.org/10.1038/s41586-018-0414-6

RNA velocity of single cells

Gioele La Manno[1,2], Ruslan Soldatov[1], Amit Zeisel[1,3], Emelie Braun[1,3], Hannah Hochgerner[1,3], Viktor Petukhov[1,4], Katja Lidschreiber[5], Maria E. Kastriti[6], Peter Lönnerberg[1,2], Alessandro Furlan[7], Jean Fan[1], Lars E. Borm[1,3], Zehua Liu[1], David van Bruggen[1], Jimin Guo[1], Xiaoling He[1], Roger Barker[1], Erik Sundström[8], Gonçalo Castelo-Branco[9], Patrick Cramer[5,6], Igor Adameyko[9], Sten Linnarsson[1,2]* & Peter V. Kharchenko[3,10]*

RNA abundance is a powerful indicator of the state of individual cells. Single-cell RNA sequencing can reveal RNA abundance with high quantitative accuracy, sensitivity and throughput[1]. However, this approach captures only a static snapshot at a point in time, posing a challenge for the analysis of time-resolved phenomena such as embryogenesis or tissue regeneration. Here we show that RNA velocity—the time derivative of the gene expression state—can be directly estimated by distinguishing between unspliced and spliced mRNAs in common single-cell RNA sequencing protocols. RNA velocity is a high-dimensional vector that predicts the future state of individual cells on a timescale of hours. We validate its accuracy in the neural crest lineage, demonstrate its use on multiple published datasets and technical platforms, reveal the branching lineage tree of the developing mouse hippocampus, and examine the kinetics of transcription in human embryonic brain. We expect RNA velocity to greatly aid the analysis of developmental lineages and cellular dynamics, particularly in humans.

During development, differentiation occurs on a timescale of hours to days, which is comparable to the typical half-life of mRNA. The relative abundance of nascent (unspliced) and mature (spliced) mRNA can be exploited to estimate the rates of gene splicing and degradation, without the need for metabolic labelling, as previously shown in bulk[2–4]. We reasoned that similar signals may be detectable in single-cell RNA sequencing (RNA-seq) data, and could reveal the rate and direction of change of the entire transcriptome during dynamic processes.

All common single-cell RNA-seq protocols rely on oligo-dT primers to enrich for polyadenylated mRNA molecules. Nevertheless, examining single-cell RNA-seq datasets based on the SMART-seq2, STRT/C1, inDrop and 10x Genomics Chromium protocols[5–8], we found that 15–25% of reads contained unspliced intronic sequences (Fig. 1a), in agreement with previous observations in bulk[9] (14.6%) and single-cell[2] (~20%) RNA-seq. Most such reads originated from secondary priming positions within the intronic regions (Extended Data Fig. 1). In 10x Genomics Chromium libraries, we also found abundant discordant priming from the more commonly occurring intronic poly(T) sequences (Extended Data Fig. 1), which may have been generated during PCR amplification by priming on the first-strand cDNA. The substantial number of intronic molecules and their correlation with the exonic counts suggest that those molecules represent unspliced precursor mRNAs. This was confirmed by metabolic labelling of newly transcribed RNA[9] followed by RNA sequencing using oligo-dT-primed single-cell-tagged reverse transcription (STRT)[10] (Extended Data Fig. 2); 85% of all genes displayed expression time courses consistent with simple first-order kinetics, as expected if unspliced reads represent nascent mRNA.

To quantify the time-dependent relationship between the abundance of precursor and mature mRNA, we assumed a simple model for transcriptional dynamics[2], in which the first-time derivative of the spliced mRNA abundance (RNA velocity) is determined by the balance between production of spliced mRNA from unspliced mRNA, and the mRNA degradation (Fig. 1b and Supplementary Note 1). Under such a model, steady states are approached asymptotically when the rate of transcription α is constant, with the steady-state abundances of spliced (s) and unspliced (u) molecules determined by α, and constrained to a fixed slope relationship where $u = \gamma s$ (Supplementary Note 2 Section 1). The equilibrium slope γ combines degradation and splicing rates, capturing gene-specific regulatory properties, the ratio of intronic and exonic lengths, and the number of internal priming sites. Using a recently published compendium of mouse tissues[11], we found that the steady-state behaviour of most genes across a wide range of cell types was consistent with a single fixed slope γ (Extended Data Fig. 3a–c). However, 11% of genes showed distinct slopes in different subsets of tissues (Extended Data Fig. 3d, e), suggesting tissue-specific alternative splicing (Extended Data Fig. 3f) or degradation rates.

During a dynamic process, an increase in the transcription rate α results in a rapid increase in unspliced mRNA, followed by a subsequent increase in spliced mRNA (Fig. 1c and Supplementary Note 2 Section 1) until a new steady state is reached. Conversely, a drop in the rate of transcription first leads to a rapid drop in unspliced mRNA, followed by a reduction in spliced mRNAs. During induction of gene expression, unspliced mRNAs are present in excess of the expectation based on the equilibrium rate γ, whereas the opposite is true during repression (Fig. 1d). The balance of unspliced and spliced mRNA abundance is, therefore, an indicator of the future state of mature mRNA abundance, and thus the future state of the cell.

To demonstrate how this simple model can be used to extrapolate the mature mRNA abundance into the future, we examined a time course of bulk RNA-seq measurements of the circadian cycle in the mouse liver[12]. Unspliced mRNA levels at each time point were consistently more similar to the spliced mRNA of the subsequent time (Fig. 1e), and many circadian-associated genes showed the expected excess of unspliced mRNA relative to the slope γ during upregulation, and a corresponding deficit during downregulation (Fig. 1f, g). Solving the proposed differential equations for each gene allowed us to extrapolate each measurement throughout the circadian cycle, accurately capturing the expected direction of progression of the circadian cycle (Fig. 1h).

Next, to demonstrate the ability to predict transcriptional dynamics in single-cell measurements, we analysed recently published single-cell mRNA-seq data of mouse chromaffin cells[7], obtained using SMART-seq2[5] (Fig. 2). During development, a substantial proportion of chromaffin cells, which are neuroendocrine cells of the adrenal medulla, arise from Schwann cell precursors, providing a convenient test case in which the direction of differentiation can be validated by lineage tracing. Phase portraits of many genes showed the expected deviations

[1]Laboratory of Molecular Neurobiology, Department of Medical Biochemistry and Biophysics, Karolinska Institutet, Stockholm, Sweden. [2]Science For Life Laboratory, Solna, Sweden. [3]Department of Biomedical Informatics, Harvard Medical School, Boston, MA, USA. [4]Department of Applied Mathematics, Peter the Great St. Petersburg Polytechnic University, St. Petersburg, Russia. [5]Department of Biosciences and Nutrition, Karolinska Institutet, Stockholm, Sweden. [6]Department of Physiology and Pharmacology, Karolinska Institutet, Stockholm, Sweden. [7]Simon Grant Centre for Brain Repair, Department of Clinical Neurosciences, University of Cambridge, Cambridge, UK. [8]Division of Neuroregeneration, Department of Neurobiology, Care Sciences and Society, Karolinska Institutet, Stockholm, Sweden. [9]Max Planck Institute for Biophysical Chemistry, Department of Molecular Biology, Göttingen, Germany. [10]Harvard Stem Cell Institute, Cambridge, MA, USA. *e-mail: sten.linnarsson@ki.se; peter_kharchenko@hms.harvard.edu

The single cell revolution

Interesting Biological Experiments

Computation

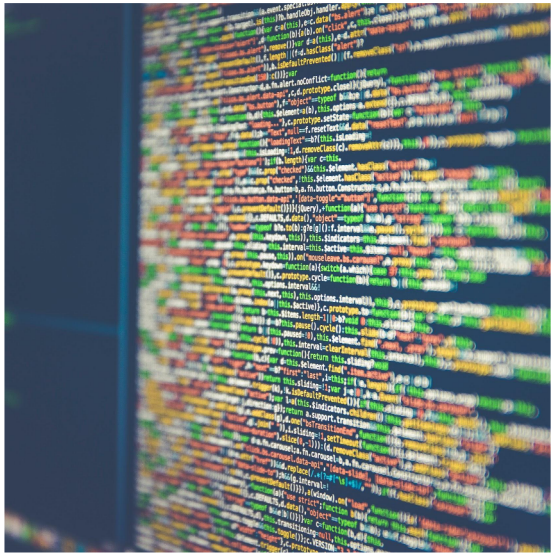

High impact paper

LETTER

https://doi.org/10.1038/s41586-018-0414-6

RNA velocity of single cells

Gioele La Manno[1,2], Ruslan Soldatov[1], Amit Zeisel[1,3], Emelie Braun[1,3], Hannah Hochgerner[1,3], Viktor Petukhov[1,4], Katja Lidschreiber[5], Maria E. Kastriti[6], Peter Lönnerberg[1,2], Alessandro Furlan[7], Jean Fan[1], Lars E. Borm[1,3], Zehua Liu[1], David van Bruggen[1], Jimin Guo[1], Xiaoling He[1], Roger Barker[1], Erik Sundström[8], Gonçalo Castelo-Branco[9], Patrick Cramer[5,6], Igor Adameyko[6], Sten Linnarsson[1,2]* & Peter V. Kharchenko[3,10]*

RNA abundance is a powerful indicator of the state of individual cells. Single-cell RNA sequencing can reveal RNA abundance with high quantitative accuracy, sensitivity and throughput[1]. However, this approach captures only a static snapshot at a point in time, posing a challenge for the analysis of time-resolved phenomena such as embryogenesis or tissue regeneration. Here we show that RNA velocity—the time derivative of the gene expression state—can be directly estimated by distinguishing between unspliced and spliced mRNAs in common single-cell RNA sequencing protocols. RNA velocity is a high-dimensional vector that predicts the future state of individual cells on a timescale of hours. We validate its accuracy in the neural crest lineage, demonstrate its use on multiple published datasets and technical platforms, reveal the branching lineage tree of the developing mouse hippocampus, and examine the kinetics of transcription in human embryonic brain. We expect RNA velocity to greatly aid the analysis of developmental lineages and cellular dynamics, particularly in humans.

During development, differentiation occurs on a timescale of hours to days, which is comparable to the typical half-life of mRNA. The relative abundance of nascent (unspliced) and mature (spliced) mRNA can be exploited to estimate the rates of gene splicing and degradation, without the need for metabolic labelling, as previously shown in bulk[2–4]. We reasoned that similar signals may be detectable in single-cell RNA sequencing (RNA-seq) data, and could reveal the rate and direction of change of the entire transcriptome during dynamic processes.

All common single-cell RNA-seq protocols rely on oligo-dT primers to enrich for polyadenylated mRNA molecules. Nevertheless, examining single-cell RNA-seq datasets based on the SMART-seq2, STRT/C1, inDrop and 10x Genomics Chromium protocols[5–8], we found that 15–25% of reads contained unspliced intronic sequences (Fig. 1a), in agreement with previous observations in bulk[9] (14.6%) and single-cell[2] (~20%) RNA-seq. Most such reads originated from secondary priming positions within the intronic regions (Extended Data Fig. 1). In 10x Genomics Chromium libraries, we also found abundant discordant priming from the more commonly occurring intronic poly(T) sequences (Extended Data Fig. 1), which may have been generated during PCR amplification by priming on the first-strand cDNA. The substantial number of intronic molecules and their correlation with the exonic counts suggest that these molecules represent unspliced precursor mRNAs. This was confirmed by metabolic labelling of newly transcribed RNA[9] followed by RNA sequencing using oligo-dT-primed single-cell-tagged reverse transcription (STRT)[10] (Extended Data Fig. 2); 85% of all genes displayed expression time courses consistent with simple first-order kinetics, as expected if unspliced reads represent nascent mRNA.

To quantify the time-dependent relationship between the abundance of precursor and mature mRNA, we assumed a simple model for transcriptional dynamics[2], in which the first time derivative of the spliced mRNA abundance (RNA velocity) is determined by the balance between production of spliced mRNA from unspliced mRNA, and the mRNA degradation (Fig. 1b and Supplementary Note 1). Under such a model, steady states are approached asymptotically when the rate of transcription α is constant, with the steady-state abundances of spliced (s) and unspliced (u) molecules determined by α, and constrained to a fixed slope relationship where $u = \gamma s$ (Supplementary Note 2 Section 1). The equilibrium slope γ combines degradation and splicing rates, capturing gene-specific regulatory properties, the ratio of intronic and exonic lengths, and the number of internal priming sites. Using a recently published compendium of mouse tissues[11], we found that the steady-state behaviour of most genes across a wide range of cell types was consistent with a single fixed slope γ (Extended Data Fig. 3a–c). However, 11% of genes showed distinct slopes in different subsets of tissues (Extended Data Fig. 3d, e), suggesting tissue-specific alternative splicing (Extended Data Fig. 3f) or degradation rates.

During a dynamic process, an increase in the transcription rate α results in a rapid increase in unspliced mRNA, followed by a subsequent increase in spliced mRNA (Fig. 1c and Supplementary Note 2 Section 1) until a new steady state is reached. Conversely, a drop in the rate of transcription first leads to a rapid drop in unspliced mRNA, followed by a reduction in spliced mRNAs. During induction of gene expression, unspliced mRNAs are present in excess of the expectation based on the equilibrium rate γ, whereas the opposite is true during repression (Fig. 1d). The balance of unspliced and spliced mRNA abundance is, therefore, an indicator of the future state of mature mRNA abundance, and thus the future state of the cell.

To demonstrate how this simple model can be used to extrapolate the mature mRNA abundance into the future, we examined a time course of bulk RNA-seq measurements of the circadian cycle in the mouse liver[12]. Unspliced mRNA levels at each time point were consistently more similar to the spliced mRNA of the subsequent time (Fig. 1e), and many circadian-associated genes showed the expected excess of unspliced mRNA relative to the slope γ during upregulation, and a corresponding deficit during downregulation (Fig. 1f, g). Solving the proposed differential equations for each gene allowed us to extrapolate each measurement throughout the circadian cycle, accurately capturing the expected direction of progression of the circadian cycle (Fig. 1h).

Next, to demonstrate the ability to predict transcriptional dynamics in single-cell measurements, we analysed recently published single-cell mRNA-seq data of mouse chromaffin cells[7], obtained using SMART-seq2[5] (Fig. 2). During development, a substantial proportion of chromaffin cells, which are neuroendocrine cells of the adrenal medulla, arise from Schwann cell precursors, providing a convenient test case in which the direction of differentiation can be validated by lineage tracing. Phase portraits of many genes showed the expected deviations

[1]Laboratory of Molecular Neurobiology, Department of Medical Biochemistry and Biophysics, Karolinska Institutet, Stockholm, Sweden. [2]Science for Life Laboratory, Solna, Sweden. [3]Department of Biomedical Informatics, Harvard Medical School, Boston, MA, USA. [4]Department of Applied Mathematics, Peter the Great St. Petersburg Polytechnic University, St. Petersburg, Russia. [5]Department of Biosciences and Nutrition, Karolinska Institutet, Stockholm, Sweden. [6]Department of Physiology and Pharmacology, Karolinska Institutet, Stockholm, Sweden. [7]Johnson Good Centre for Brain Repair, Department of Clinical Neurosciences, University of Cambridge, Cambridge, UK. [8]Division of Neuroregeneration, Department of Neurobiology, Care Sciences and Society, Karolinska Institutet, Stockholm, Sweden. [9]Max Planck Institute for Biophysical Chemistry, Department of Molecular Biology, Göttingen, Germany. [10]Harvard Stem Cell Institute, Cambridge, MA, USA. *e-mail: sten.linnarsson@ki.se; peter_kharchenko@hms.harvard.edu

- Machine learning
- Linear algebra
- Probability theory
- Statistical analysis
- Algorithm design

It's all Greek to me...

Definition 1. *The* t-step **potential distance** *is defined as* $\mathfrak{V}^t(x,y) \triangleq \|U_x^t - U_y^t\|_2$, $x, y \in \mathcal{X}$.

The following proposition shows a relation between the two metrics by expressing the potential distance in embedded diffusion map coordinates[1] for fixed-bandwidth Gaussian-based diffusion (i.e., generated by P_ε from Eq. 2):

Proposition 1. *Given a diffusion process defined by a fixed-bandwidth Gaussian kernel, the potential distance from Def 1 can be written as* $\mathfrak{V}^t(x,y) = \left(\sum_{z\in\mathcal{X}} \log^2\left(\frac{1+\left\langle\Phi^{t/2}(x),\Phi^{t/2}(z)\right\rangle}{1+\left\langle\Phi^{t/2}(y),\Phi^{t/2}(z)\right\rangle}\right)\right)^{1/2}$

Proof. According to the spectral theorem, the entries of P_ε^t can be written as

$$[P_\varepsilon^t]_{(x,y)} = \psi_0(y) + \sum_{i=1}^{n-1} \lambda_i^t \phi_i(x)\psi_i(y)$$

since powers of the operator P_ε only affect the eigenvalues, which are taken to the same power, and since the trivial eigenvalue λ_0 is one and the corresponding right eigenvector ϕ_0 only consists of ones. Furthermore, it can be verified that the left and right eigenvectors of P_ε are related by $\psi_i(y) = \phi_i(y)\psi_0(y)$, thus, combined with Eqs. 4 and 6, we get

$$p_{\varepsilon,x}^t(y) = \psi_0(y)\left(1 + \sum_{i=1}^{n-1} \lambda_i^t \phi_i(x)\phi_i(y)\right) = \psi_0(y)\left(1 + \left\langle \Phi_\varepsilon^{t/2}(x), \Phi_\varepsilon^{t/2}(x)\right\rangle\right) .$$

By applying the logarithm to both ends of this equation we express the entries of the potential representation $U_{\varepsilon,x}^t$ as

$$U_{\varepsilon,x}^t(y) = -\log(1 + \left\langle \Phi_\varepsilon^{t/2}(x), \Phi_\varepsilon^{t/2}(y)\right\rangle) - \log(\psi_0(y)) ,$$

and thus for any $j = 1, \ldots, N$,

$$\begin{aligned}\left(U_{\varepsilon,x}^t(x_j) - U_{\varepsilon,y}^t(x_j)\right)^2 &= \left[\log(1 + \left\langle \Phi_\varepsilon^{t/2}(x), \Phi_\varepsilon^{t/2}(x_j)\right\rangle)\right. \\ &- \left.\log(1 + \left\langle \Phi_\varepsilon^{t/2}(y), \Phi_\varepsilon^{t/2}(x_j)\right\rangle)\right]^2 \\ &= \log^2\left(\frac{1 + \left\langle \Phi_\varepsilon^{t/2}(x), \Phi_\varepsilon^{t/2}(x_j)\right\rangle}{1 + \left\langle \Phi_\varepsilon^{t/2}(y), \Phi_\varepsilon^{t/2}(x_j)\right\rangle}\right) ,\end{aligned}$$

which yields the result in the proposition. □

Moon et al. (2019)

What reading single cell methods can feel like

What is machine learning?

What is machine learning?

Machine learning is the process of identifying patterns in data.

Two kinds of machine learning

Supervised learning

- Have a bunch of labelled data, want to label new data

Two kinds of machine learning

Supervised learning

- Have a bunch of labelled data, want to label new data

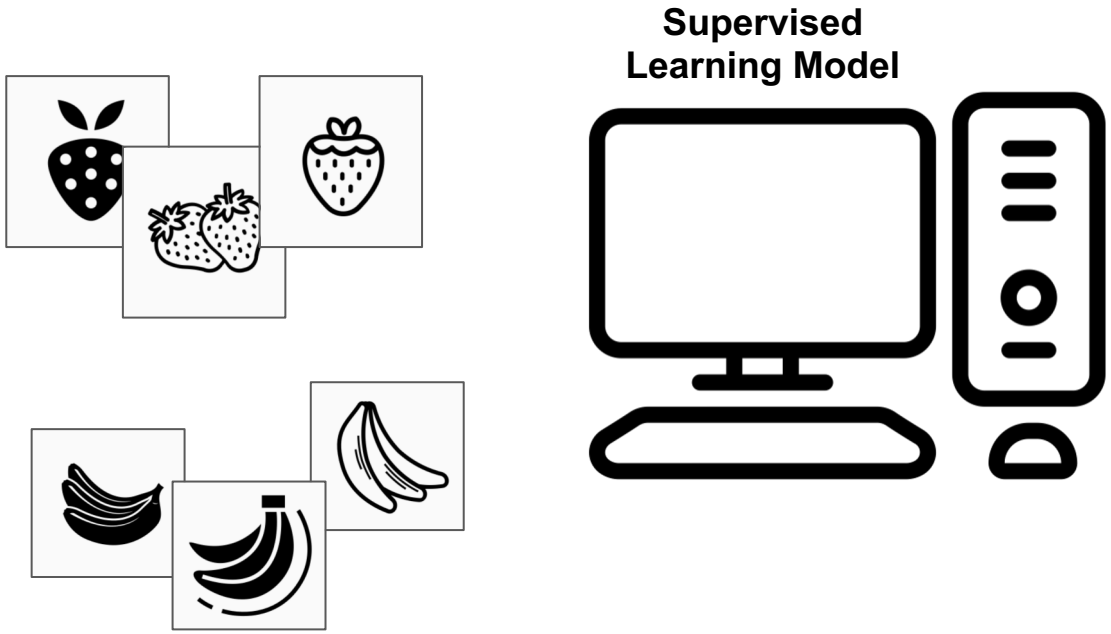

Noun project

Two kinds of machine learning

Supervised learning

- Have a bunch of labelled data, want to label new data

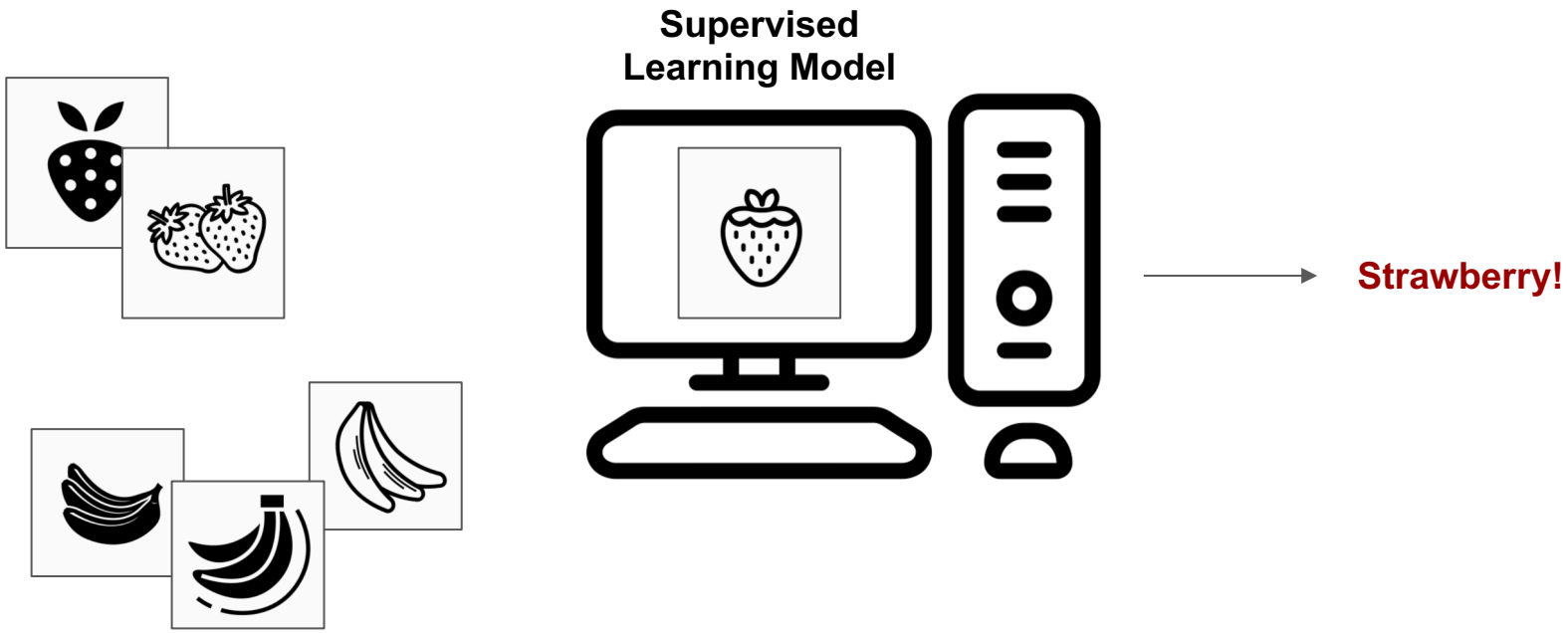

Noun project

Two kinds of machine learning

Supervised learning

- Have a bunch of labelled data, want to label new data

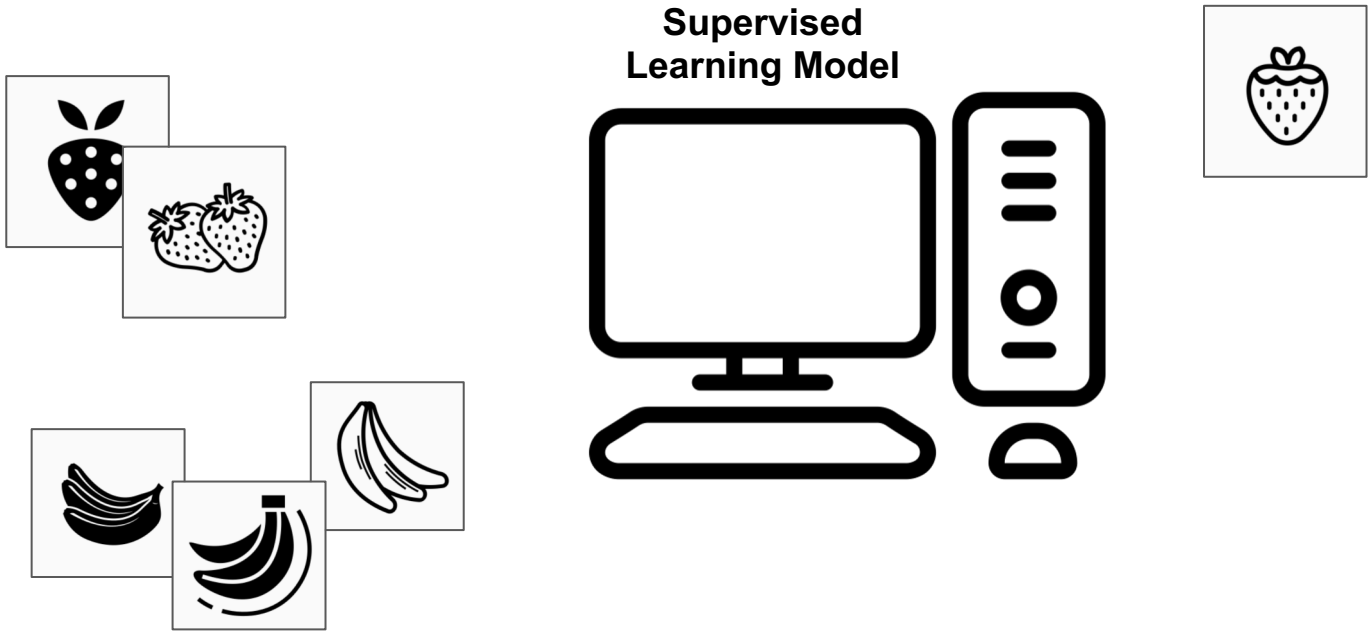

Noun project

Two kinds of machine learning

Supervised learning

- Have a bunch of labelled data, want to label new data

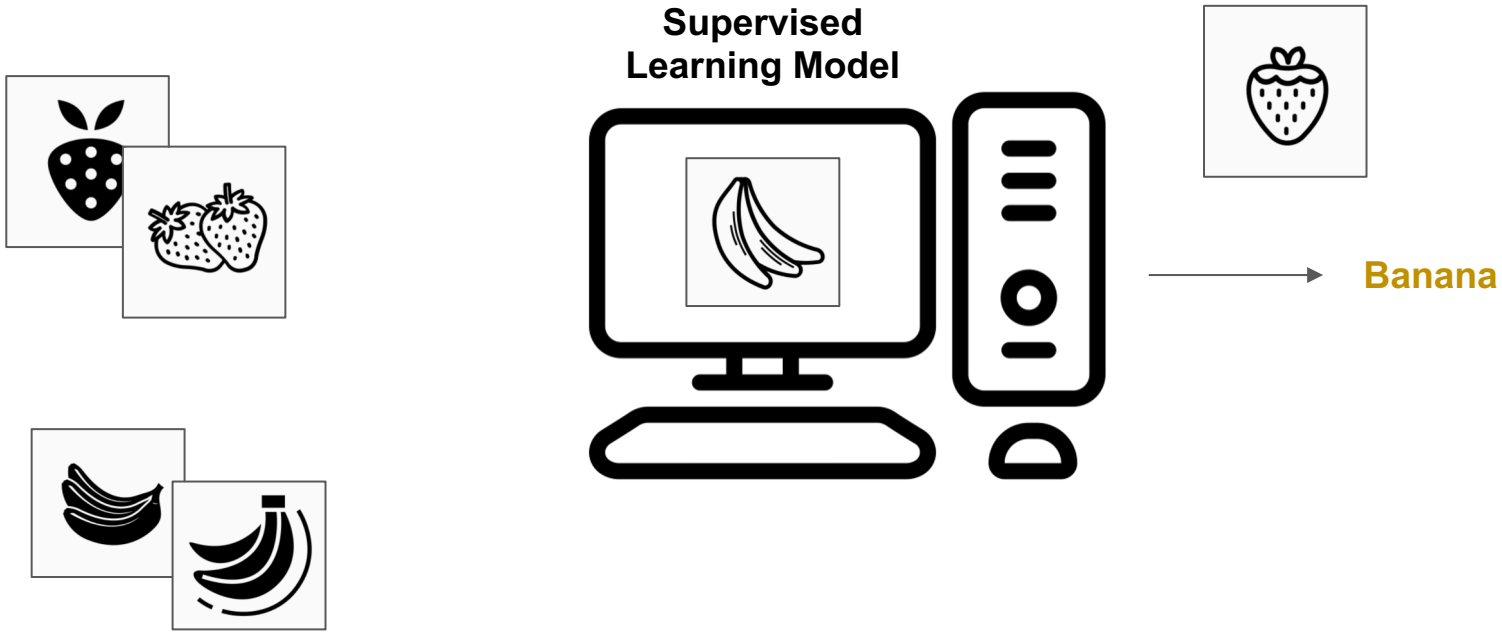

Noun project

Two kinds of machine learning

Supervised learning

- Have a bunch of labelled data, want to label new data

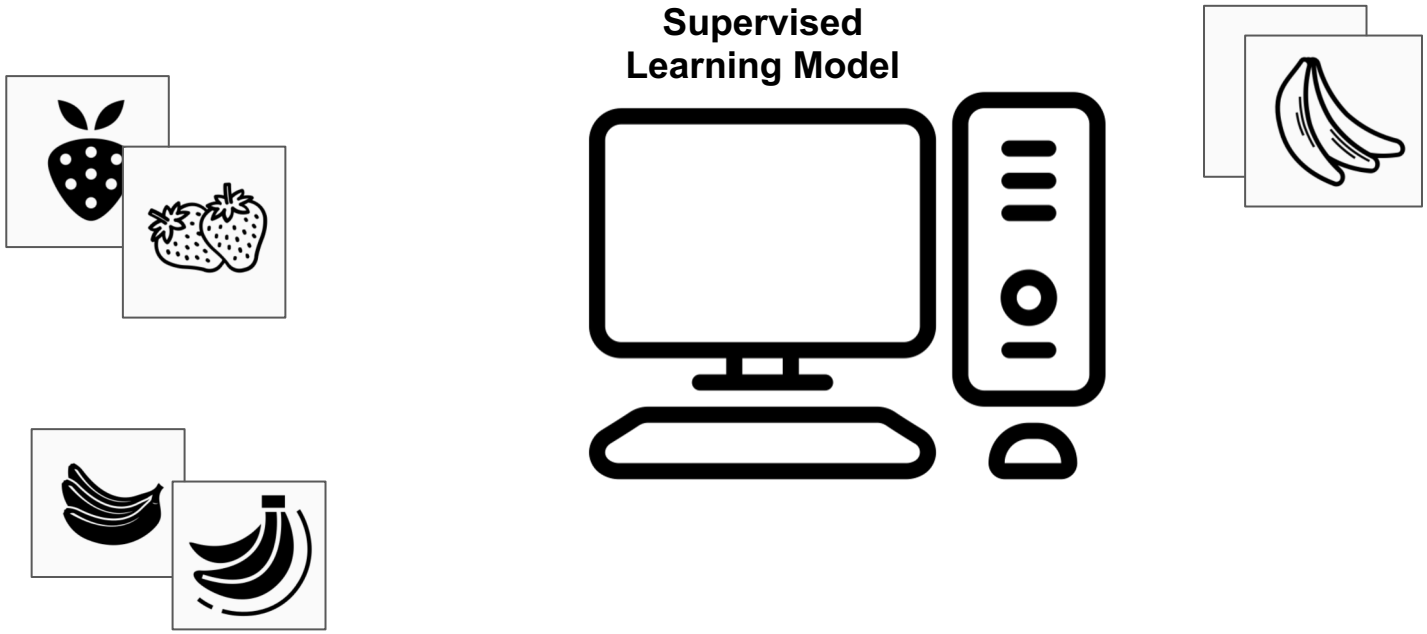

Noun project

Two kinds of machine learning

Supervised learning

- Have a bunch of labelled data, want to label new data

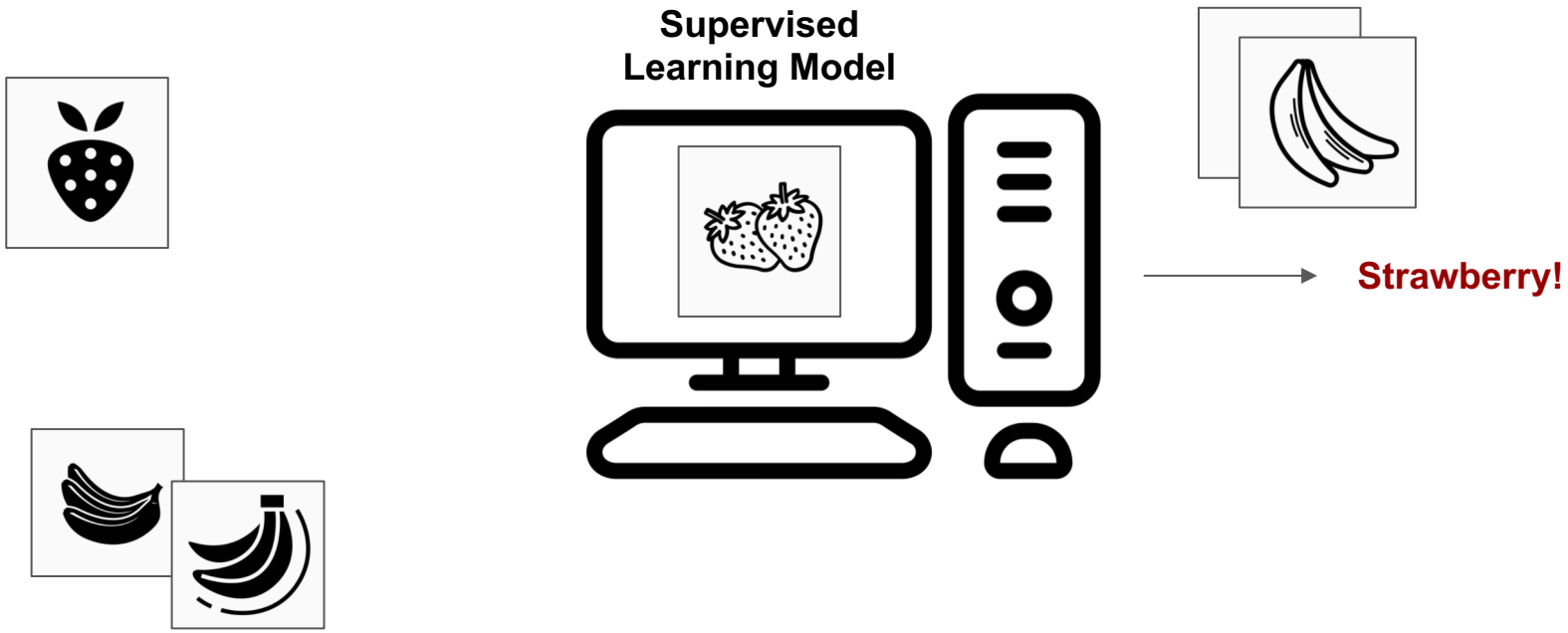

Noun project

Two kinds of machine learning

Supervised learning

- Have a bunch of labelled data, want to label new data

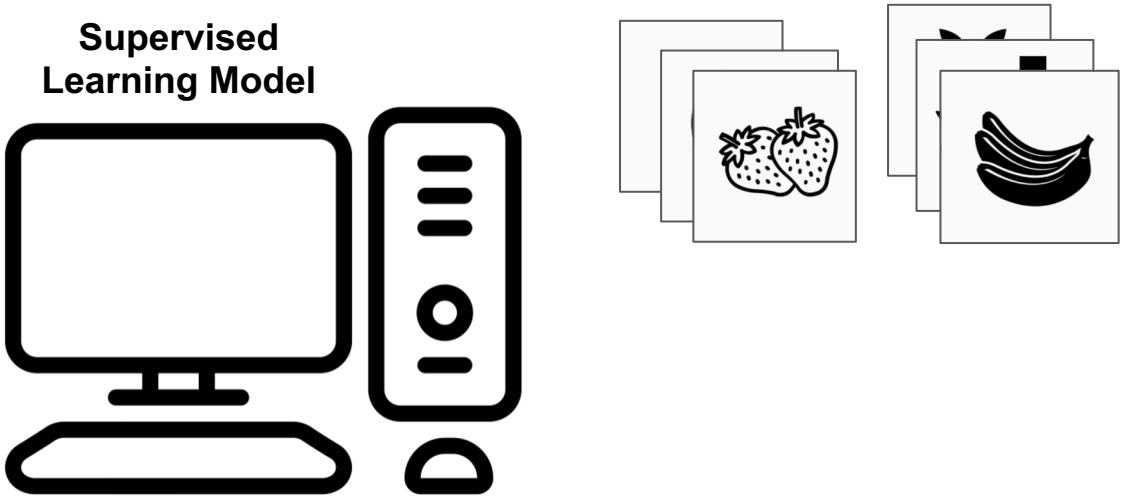

Noun project

Two kinds of machine learning

Supervised learning

- Have a bunch of labelled data, want to label new data

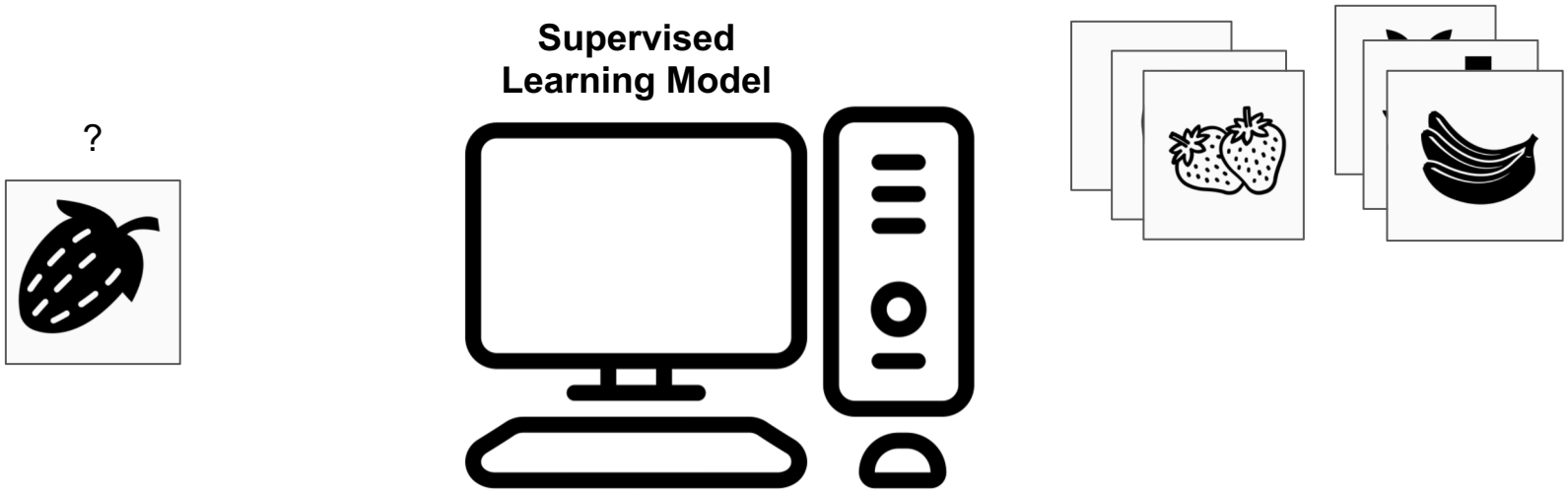

Noun project

Two kinds of machine learning

Supervised learning

- Have a bunch of labelled data, want to label new data

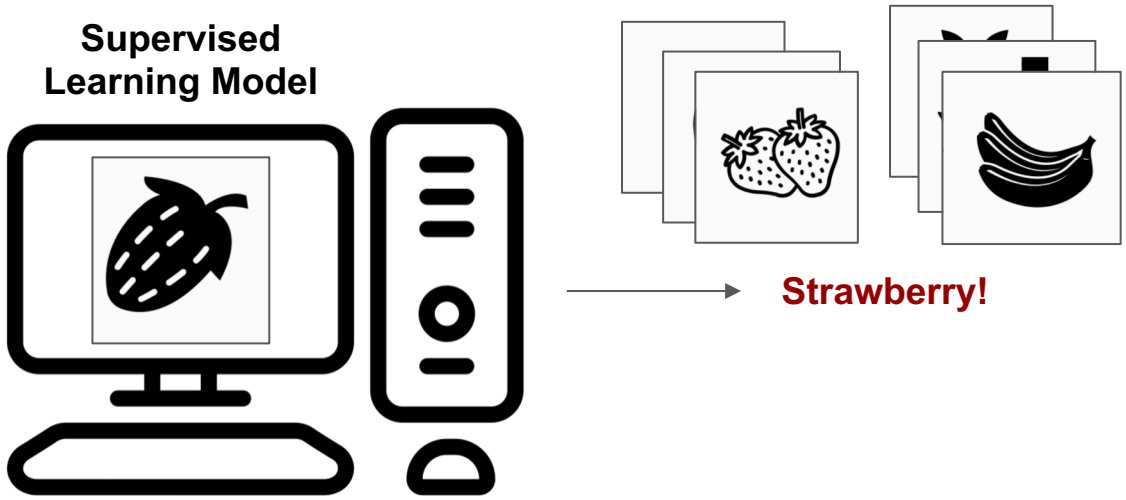

Noun project

Two kinds of machine learning

Supervised learning

- Have a bunch of labelled data, want to label new data

Unsupervised learning

- Have a bunch of unlabeled data, want to organize it

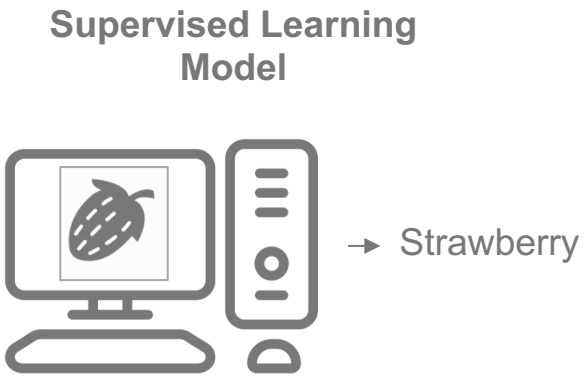

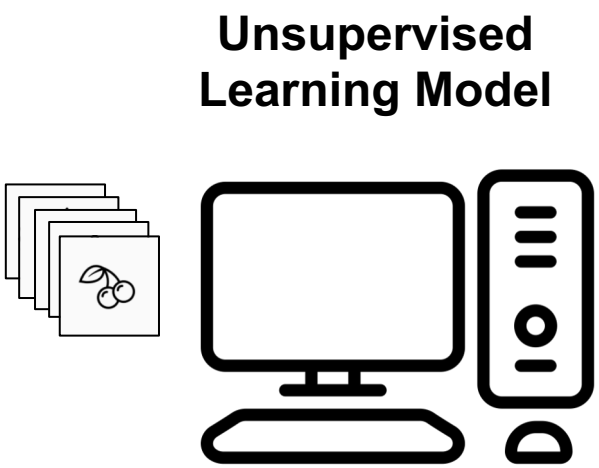

Noun project

Two kinds of machine learning

Supervised learning

- Have a bunch of labelled data, want to label new data

Unsupervised learning

- Have a bunch of unlabeled data, want to organize it

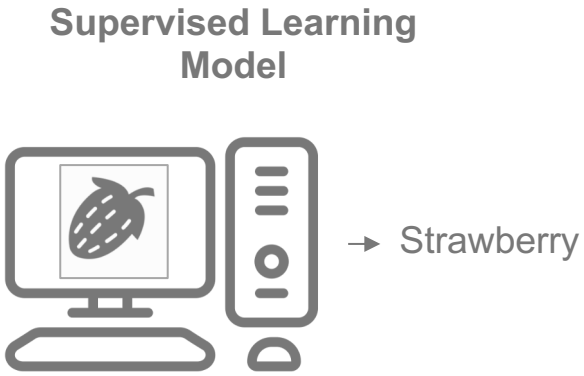

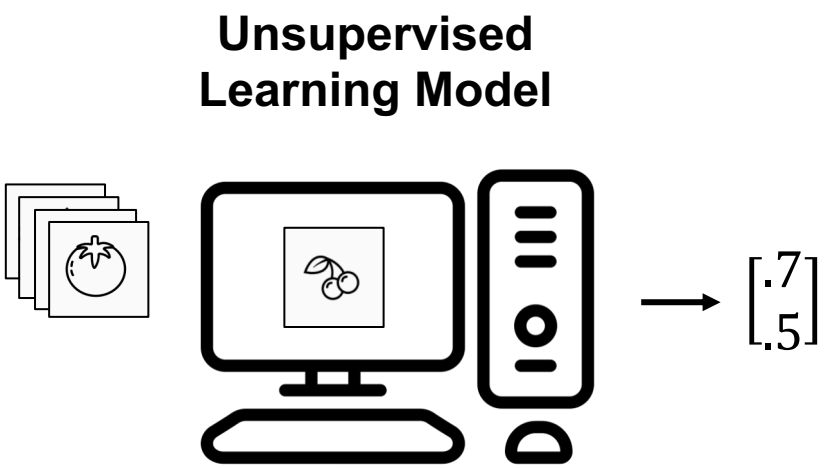

Noun project

Two kinds of machine learning

Supervised learning

- Have a bunch of labelled data, want to label new data

Unsupervised learning

- Have a bunch of unlabeled data, want to organize it

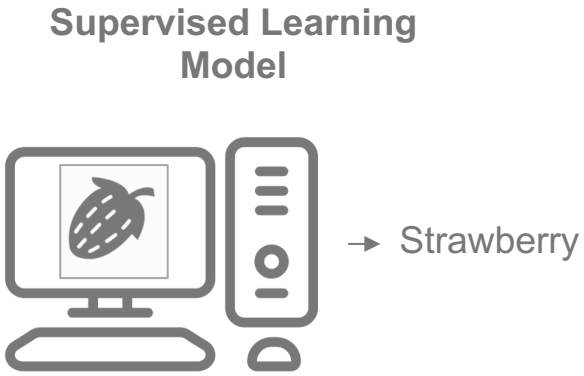

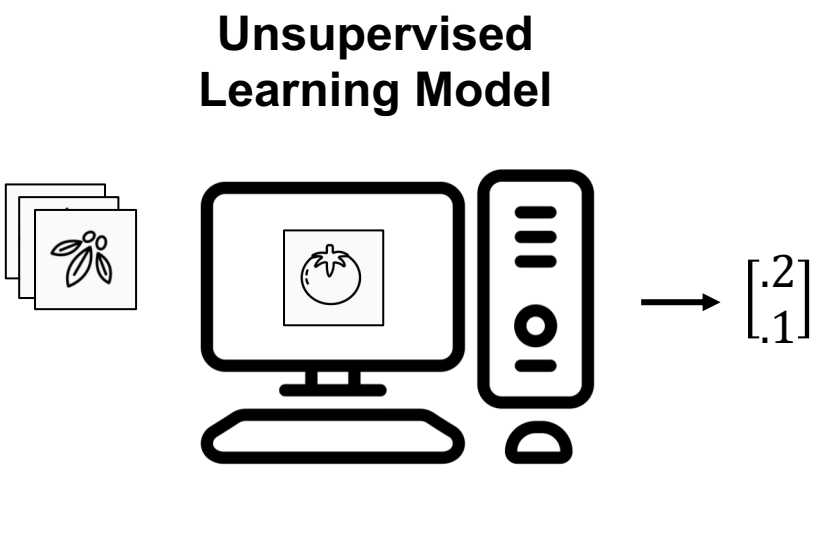

Noun project

Two kinds of machine learning

Supervised learning

- Have a bunch of labelled data, want to label new data

Unsupervised learning

- Have a bunch of unlabeled data, want to organize it

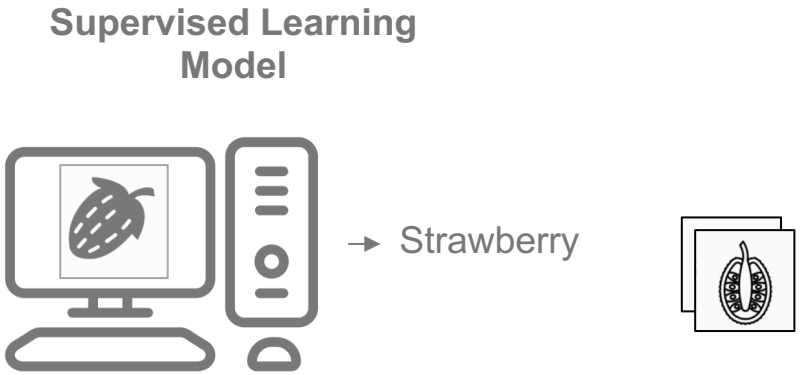

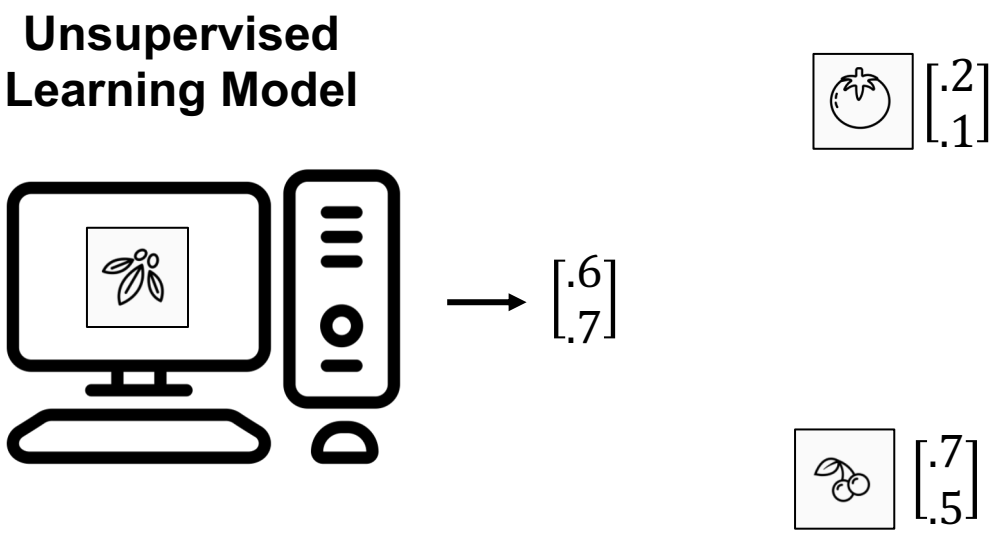

Noun project

Two kinds of machine learning

Supervised learning

- Have a bunch of labelled data, want to label new data

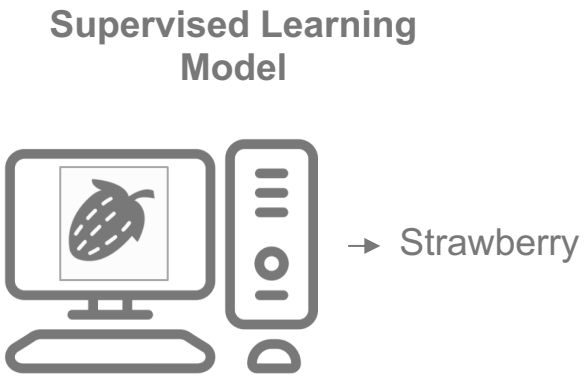

Unsupervised learning

- Have a bunch of unlabeled data, want to organize it

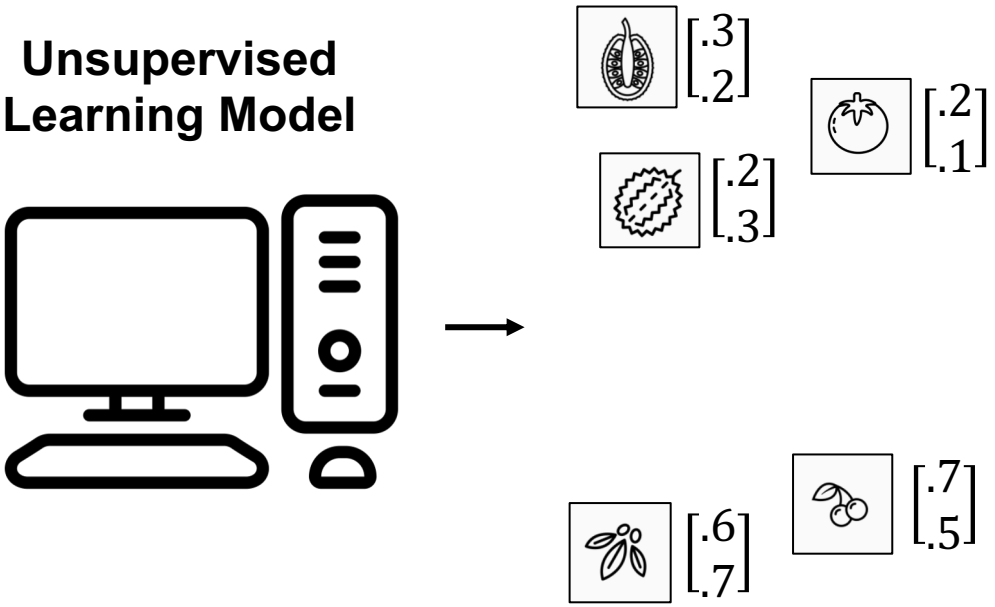

Noun project

Two kinds of machine learning

Supervised learning

- Have a bunch of labelled data, want to label new data
- Learn a function $f(X) \rightarrow Y$ where all values of Y are known for some samples of X

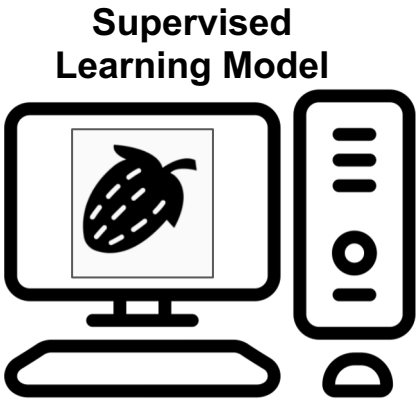

Unsupervised learning

- Have a bunch of unlabeled data, want to organize it
- Learn an embedding $f(X) \rightarrow Y, X \in \mathbb{R}^n, X \in \mathbb{R}^m, n \gg m$
- Lower dimensional, easier to interpret (e.g. as clusters)

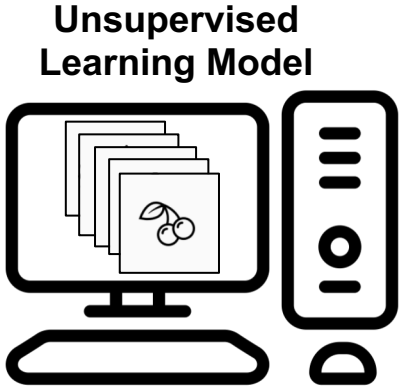

Noun project

Is linear regression an example of supervised or unsupervised machine learning?

Supervised machine learning

Unsupervised machine learning

Is clustering an example of supervised or unsupervised machine learning?

Supervised machine learning **A**

Unsupervised machine learning **B**

Course Schedule

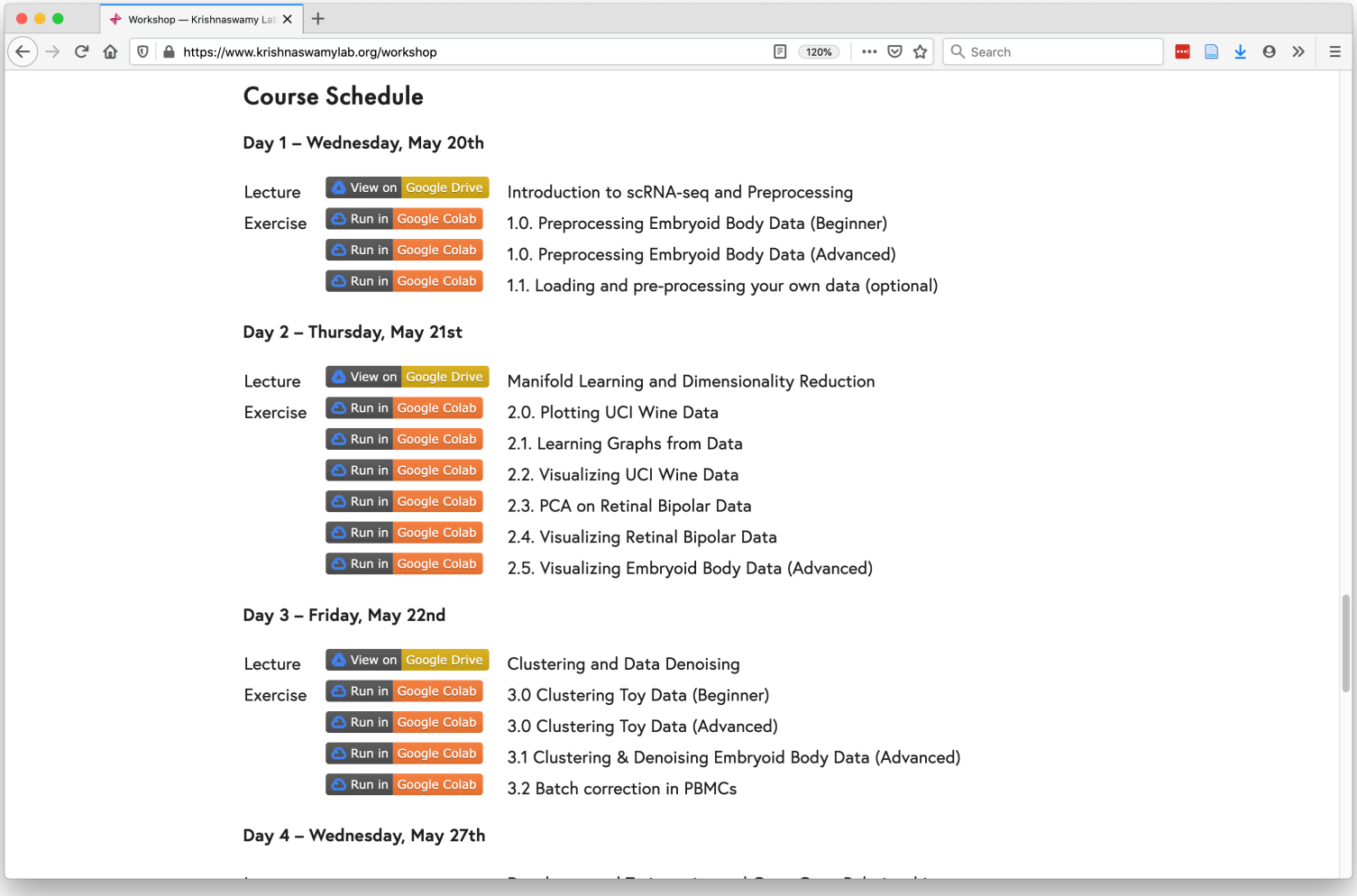

https://www.krishnaswamylab.org/workshop

Why Python?

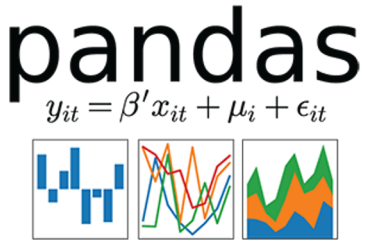

Why Python?

Tensorflow

Pytorch

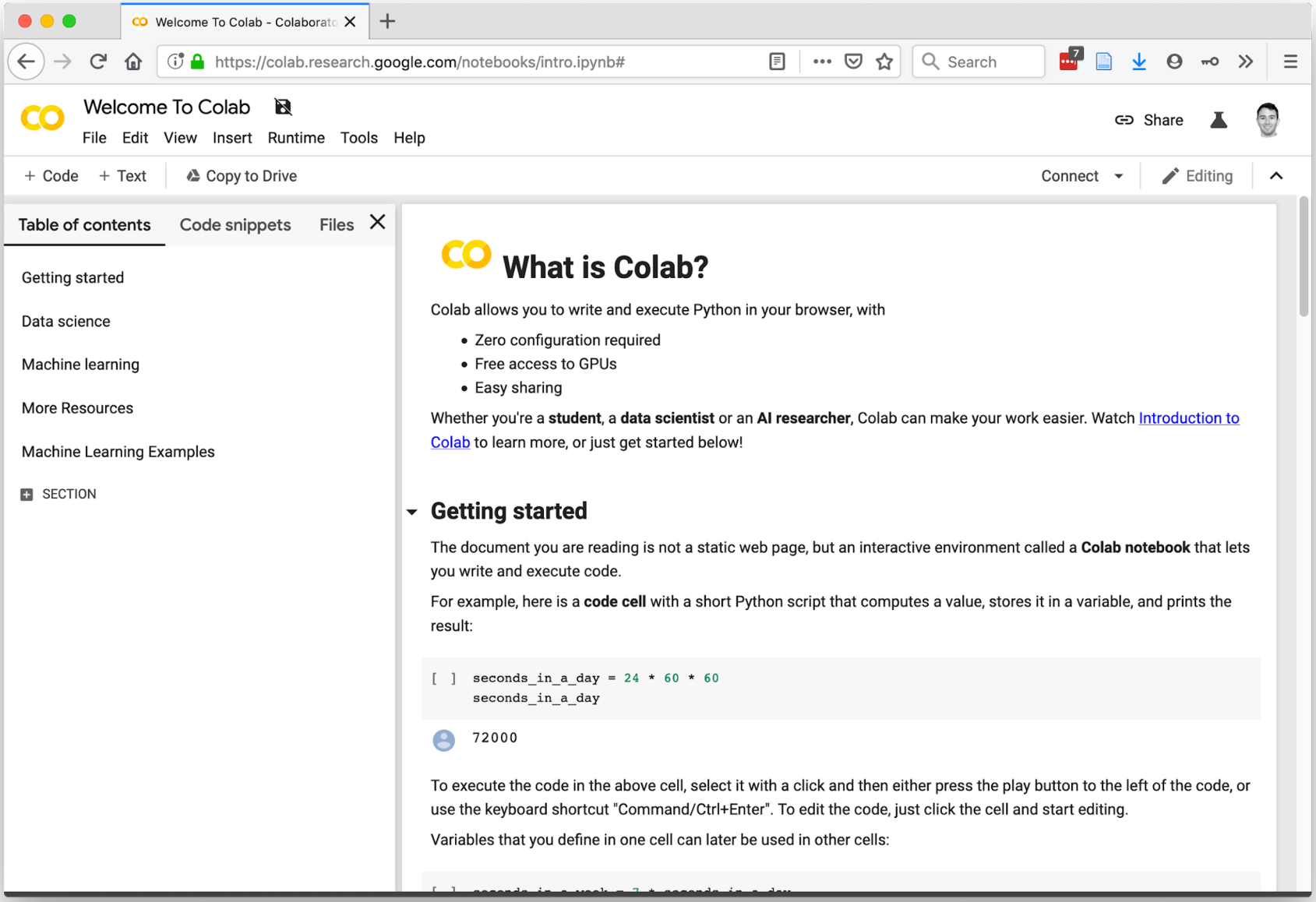

https://research.google.com/colaboratory/faq.html

Team programming

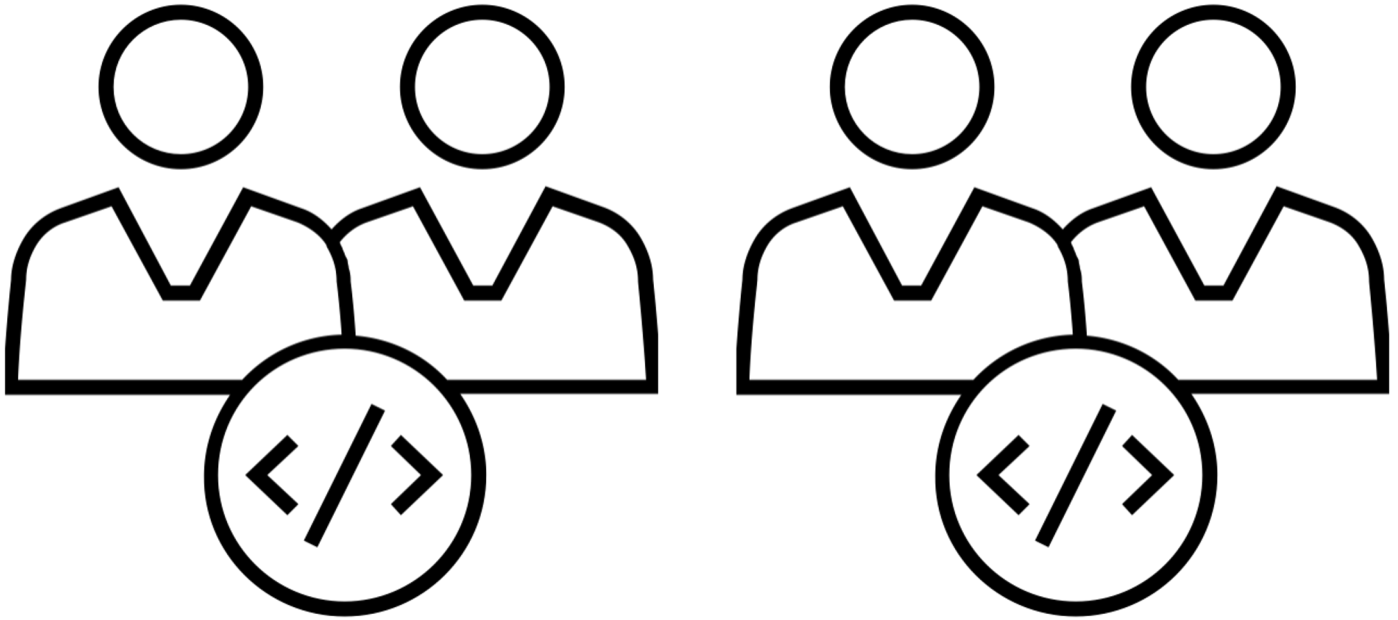

Noun project

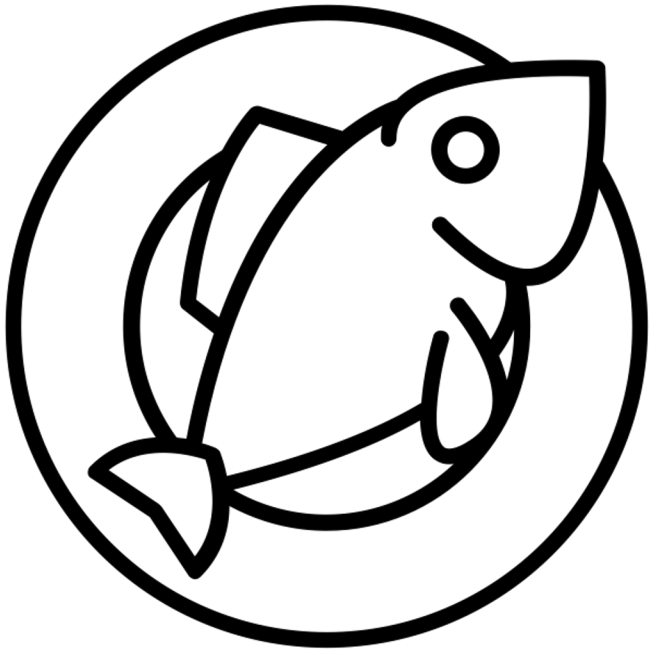

vs.

Noun project

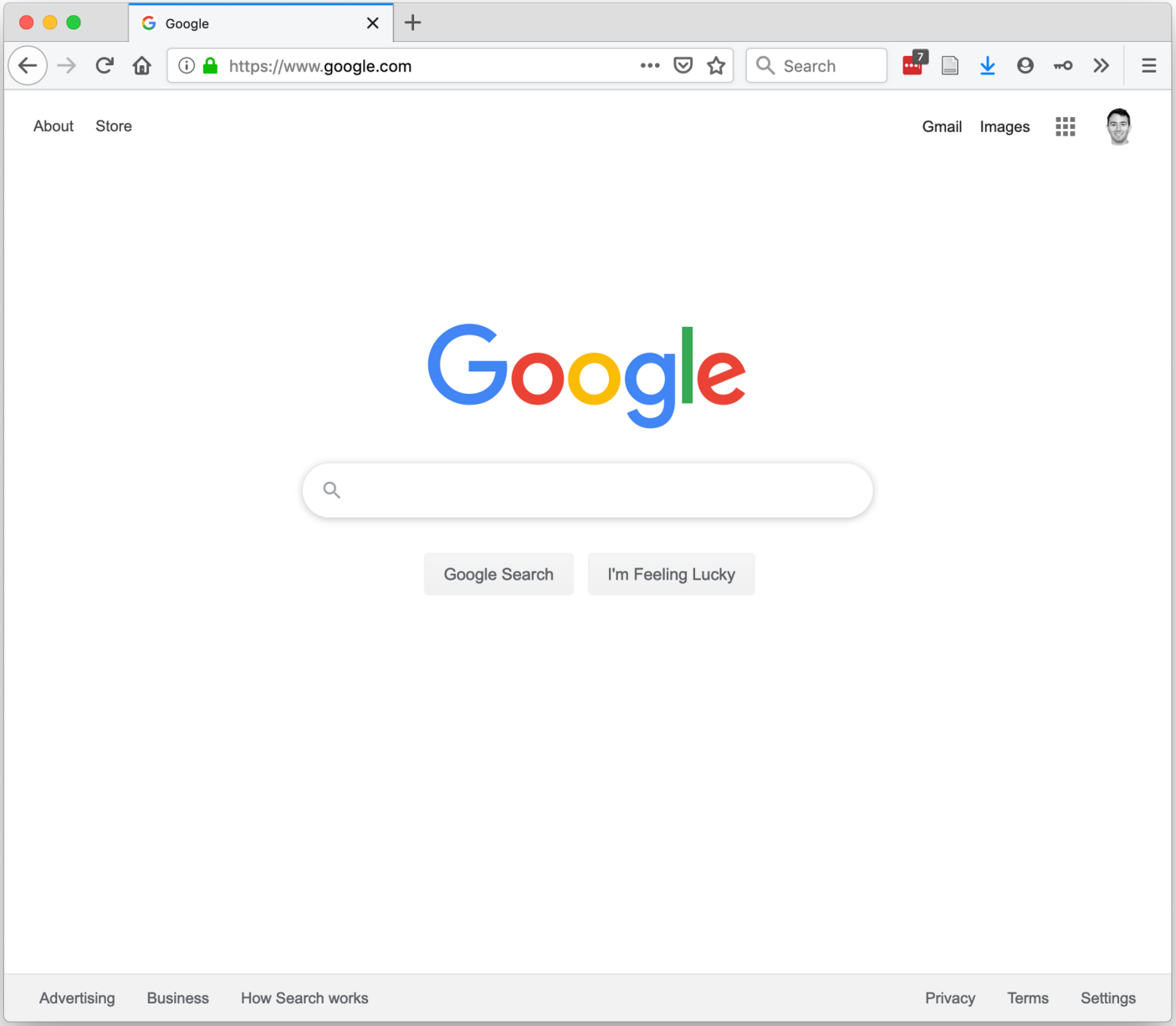
Google
https://www.google.com
Search
About
Store
Gmail
Images
Google
Google Search
I'm Feeling Lucky
Advertising
Business
How Search works
Privacy
Terms
Settings

scprep.io.load_10X(*data_dir, sparse=True, gene_labels='symbol', allow_duplicates=None*) [source]

Basic IO for 10X data produced from the 10X Cellranger pipeline.

A default run of the *cellranger count* command will generate gene-barcode matrices for secondary analysis. For both "raw" and "filtered" output, directories are created containing three files: 'matrix.mtx', 'barcodes.tsv', 'genes.tsv'. Running *scprep.io.load_10X(data_dir)* will return a Pandas DataFrame with genes as columns and cells as rows.

Parameters:

- **data_dir** (*string*) – path to input data directory expects 'matrix.mtx', 'genes.tsv', 'barcodes.tsv' to be present and will raise an error otherwise
- **sparse** (*boolean*) – If True, a sparse Pandas DataFrame is returned.
- **gene_labels** (*string, {'id', 'symbol', 'both'} optional, default: 'symbol'*) – Whether the columns of the dataframe should contain gene ids or gene symbols. If 'both', returns symbols followed by ids in parentheses.
- **allow_duplicates** (*bool, optional (default: None)*) – Whether or not to allow duplicate gene names. If None, duplicates are allowed for dense input but not for sparse input.

Returns: **data** – If sparse, data will be a pd.DataFrame[pd.SparseArray]. Otherwise, data will be a pd.DataFrame.

Return type: array-like, shape=[n_samples, n_features]

scprep.io.load_10X_HDF5(*filename, genome=None, sparse=True, gene_labels='symbol', allow_duplicates=None, backend=None*) [source]

Basic IO for HDF5 10X data produced from the 10X Cellranger pipeline.

Bring-your-own-data workshop

#2020-workshop-byod-help

https://krishnaswamylab.org/get-help

Noun project

Challenges and Opportunities in Single Cell Data

Droplet-based Technologies

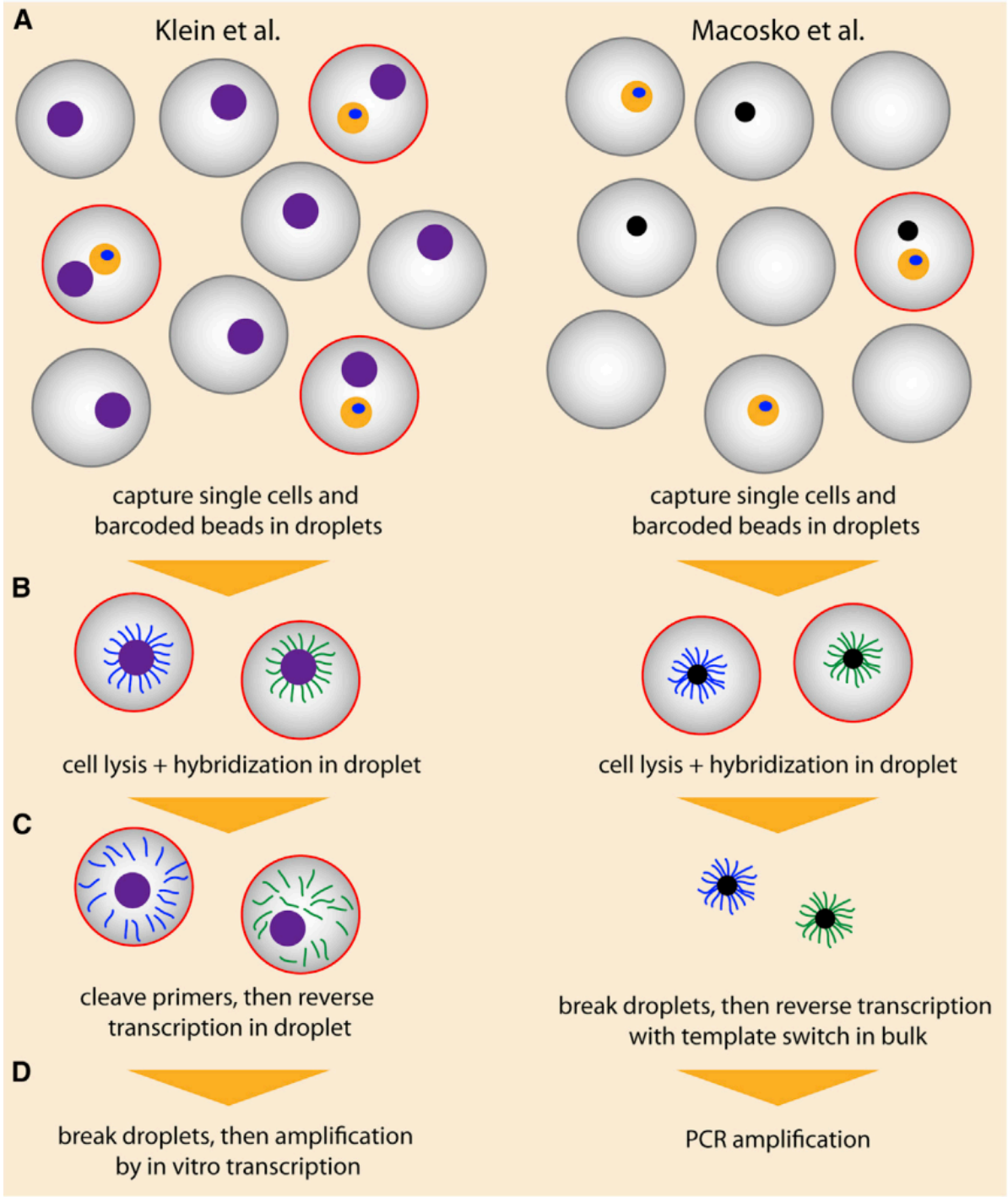

Single-Cell Proteomics: Mass Cytometry

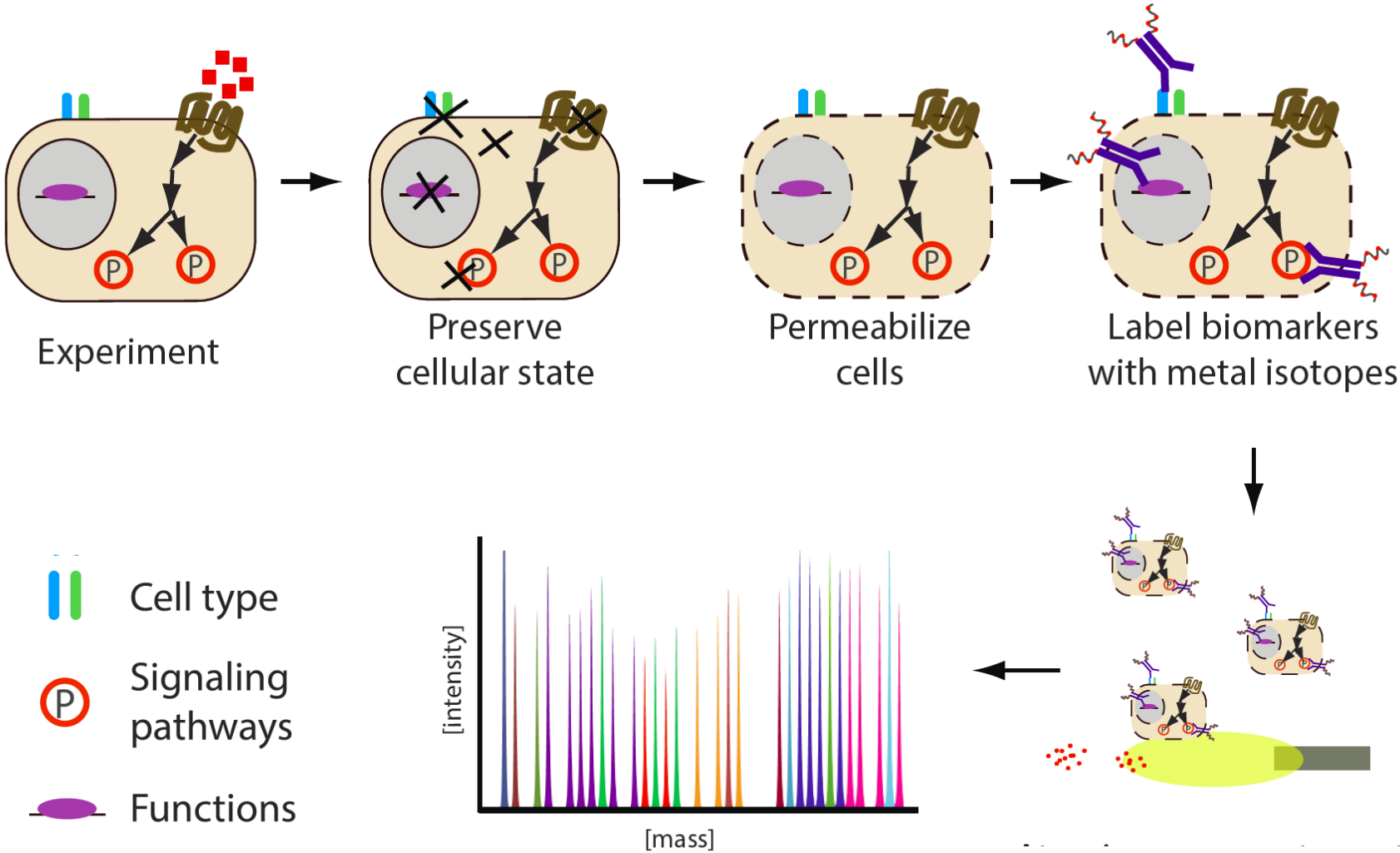

Targeted & non-redundant

MASS CYTOMETRY

Single Cell Data

- Each cell is a vector of measurements
  - e.g. Cell A = [40 0 20 18 5 0 …]
- The whole data is a matrix with many observations (cells) and features (proteins, genes)

Features
(e.g. genes)

Observations
(e.g. cells)

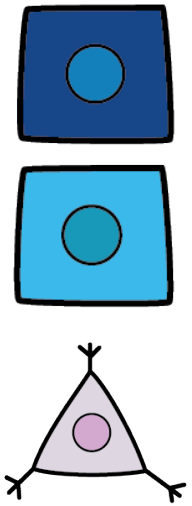

	X	Y	Z
A	10	20	70
B	20	40	140
C	20	0	80

Single Cell Data

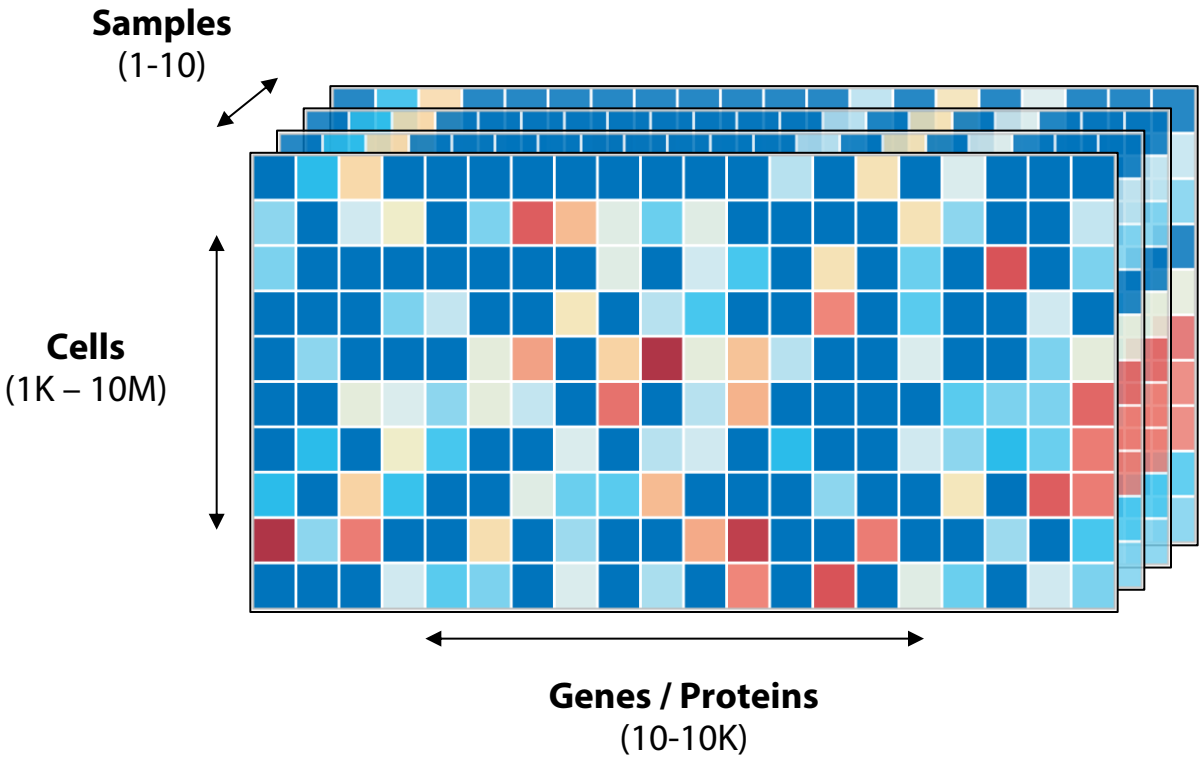

High Dimensional

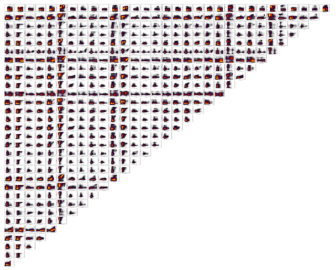

High Throughput

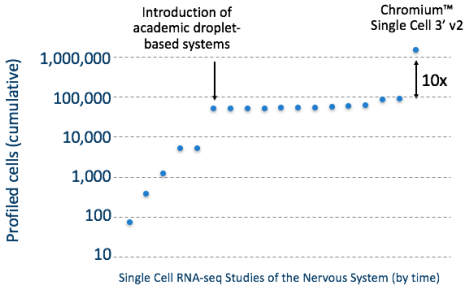

Heterogeneous

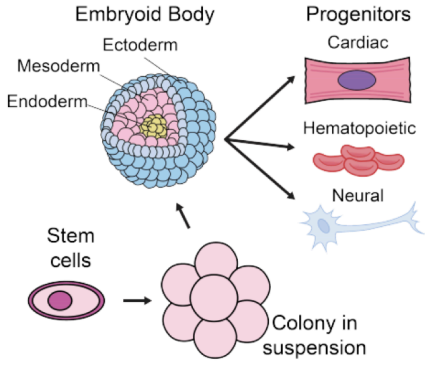

Many dimensions = many measurements

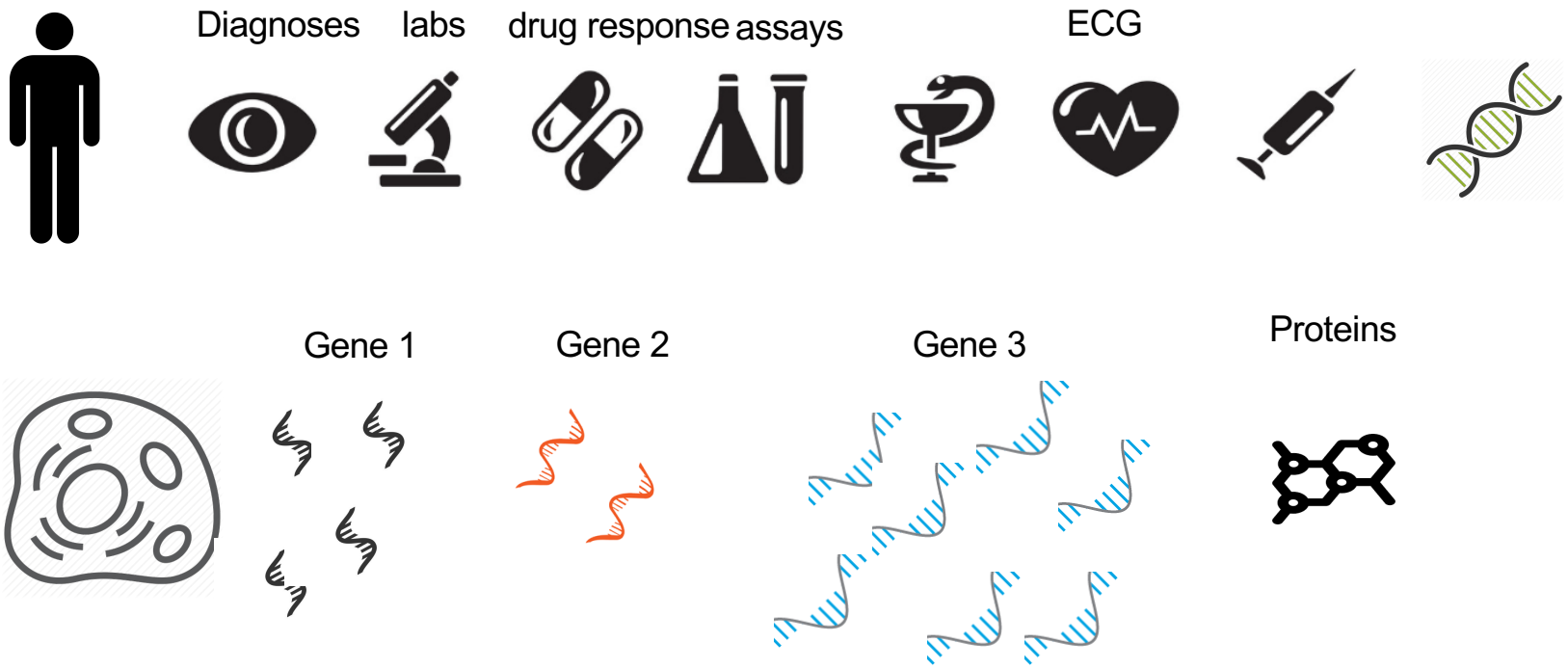

High Throughput = Many observations

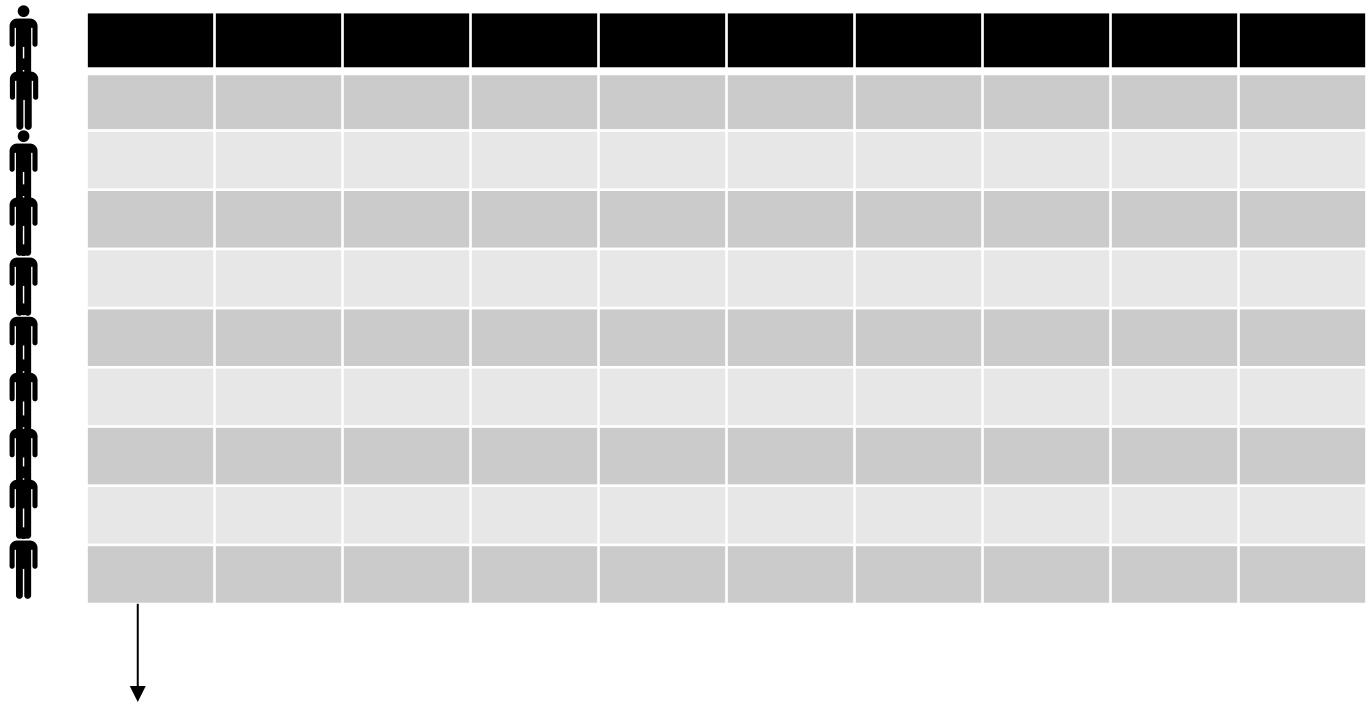

Heterogeneous Observations

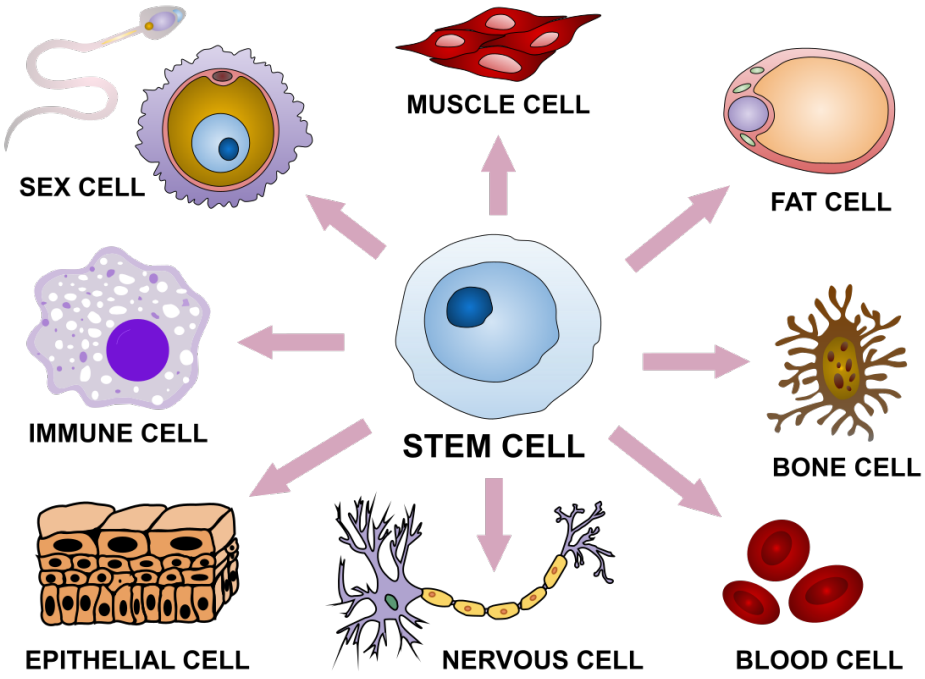

Challenges

Noise

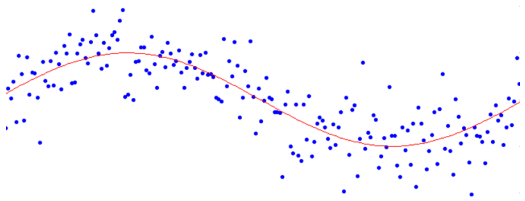

Batch Effects

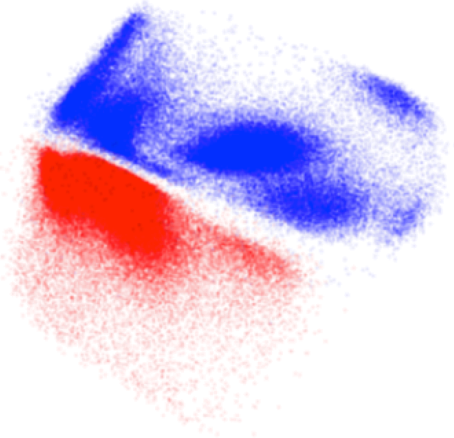

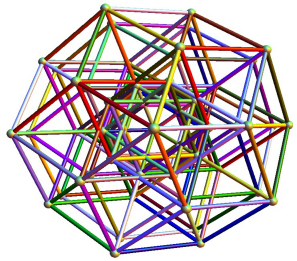

Dimensionality

Scale

Noise

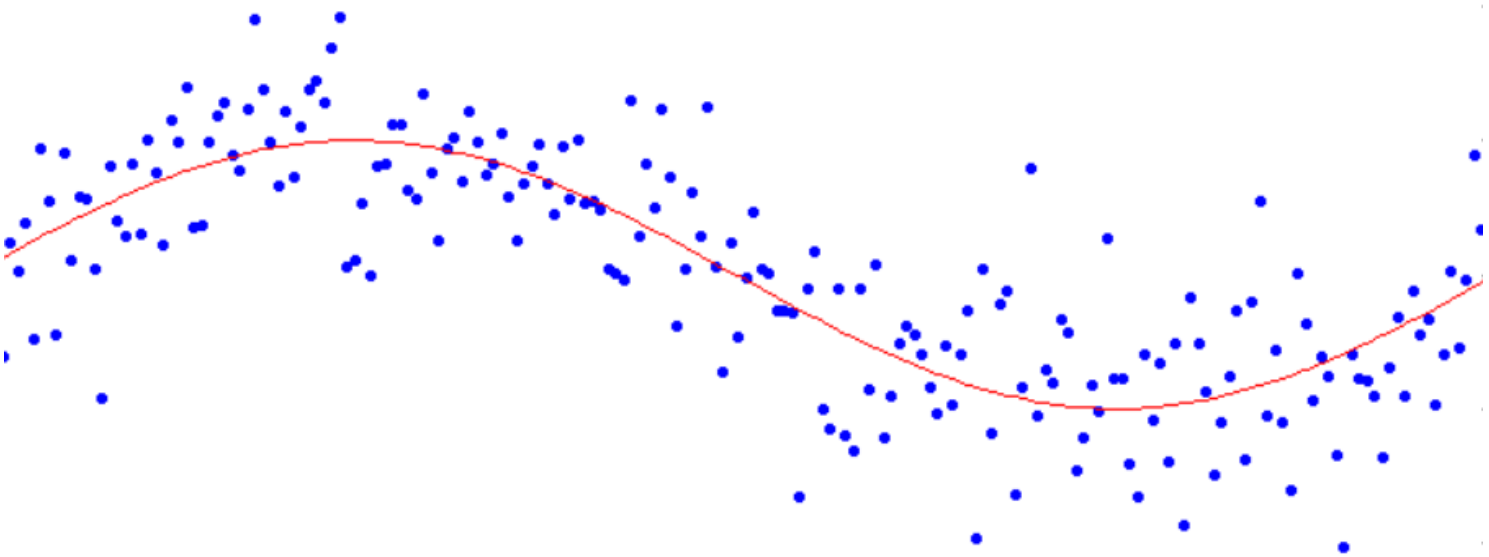

Dropout

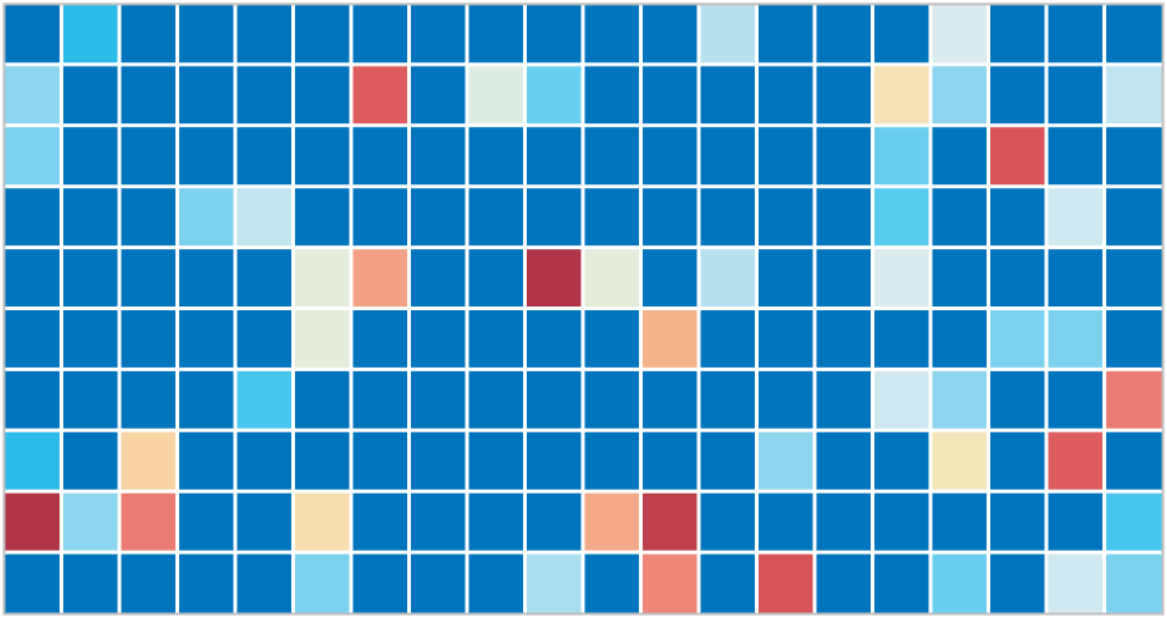

Dropout vs Missing Data

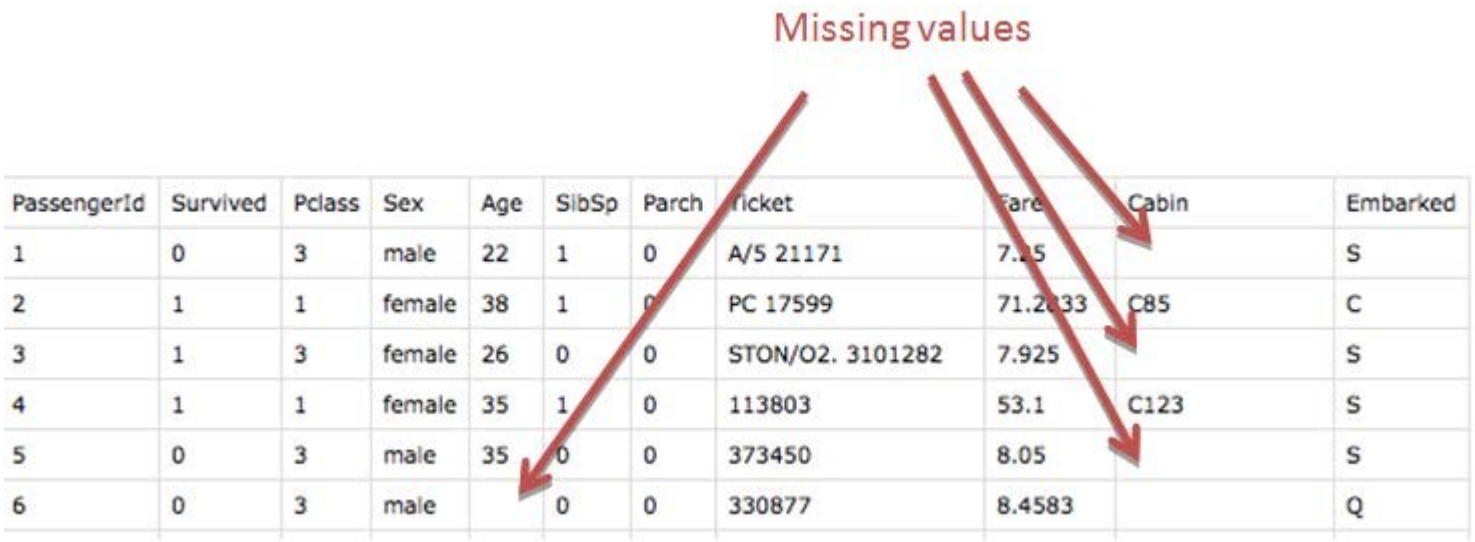

PassengerId	Survived	Pclass	Sex	Age	SibSp	Parch	Ticket	Fare	Cabin	Embarked
1	0	3	male	22	1	0	A/5 21171	7.25		S
2	1	1	female	38	1	0	PC 17599	71.2833	C85	C
3	1	3	female	26	0	0	STON/O2. 3101282	7.925		S
4	1	1	female	35	1	0	113803	53.1	C123	S
5	0	3	male	35	0	0	373450	8.05		S
6	0	3	male		0	0	330877	8.4583		Q

Denoising Data

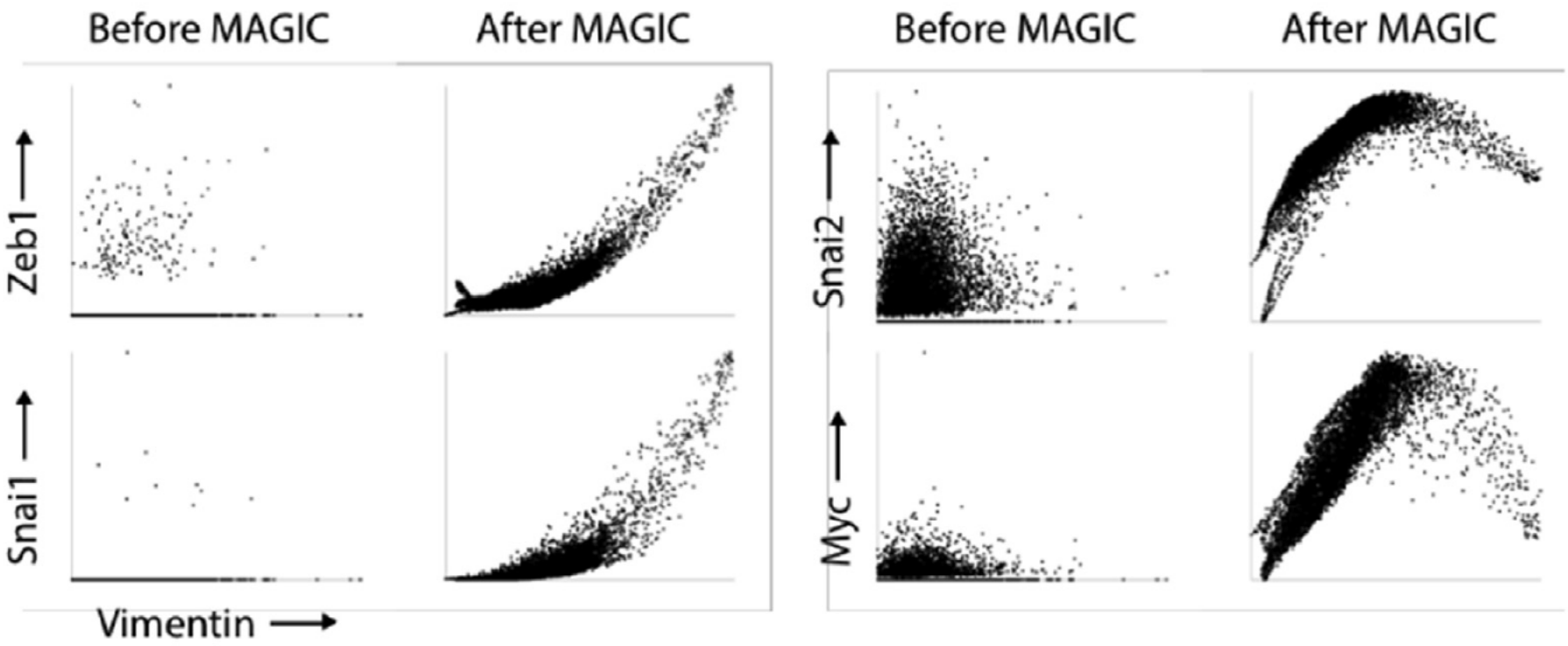

Batch Effects

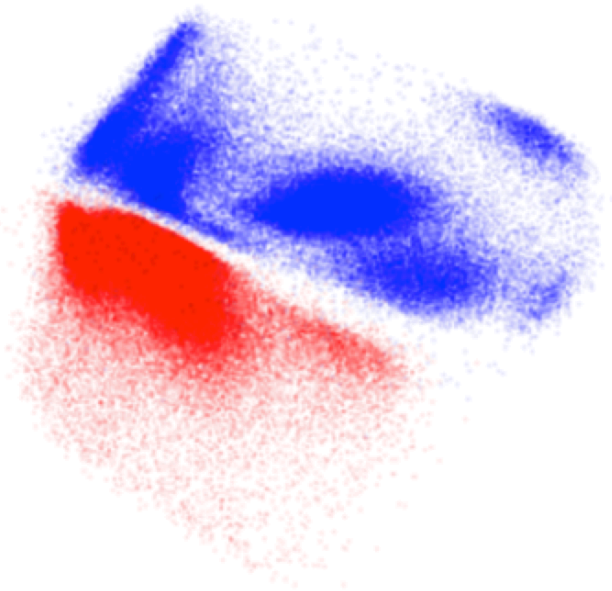

- Systematic differences between samples due to machine calibration, ambient environmental effects
- Variation that is uninteresting to examine and confounds biological variation
- Renders samples uncomparable

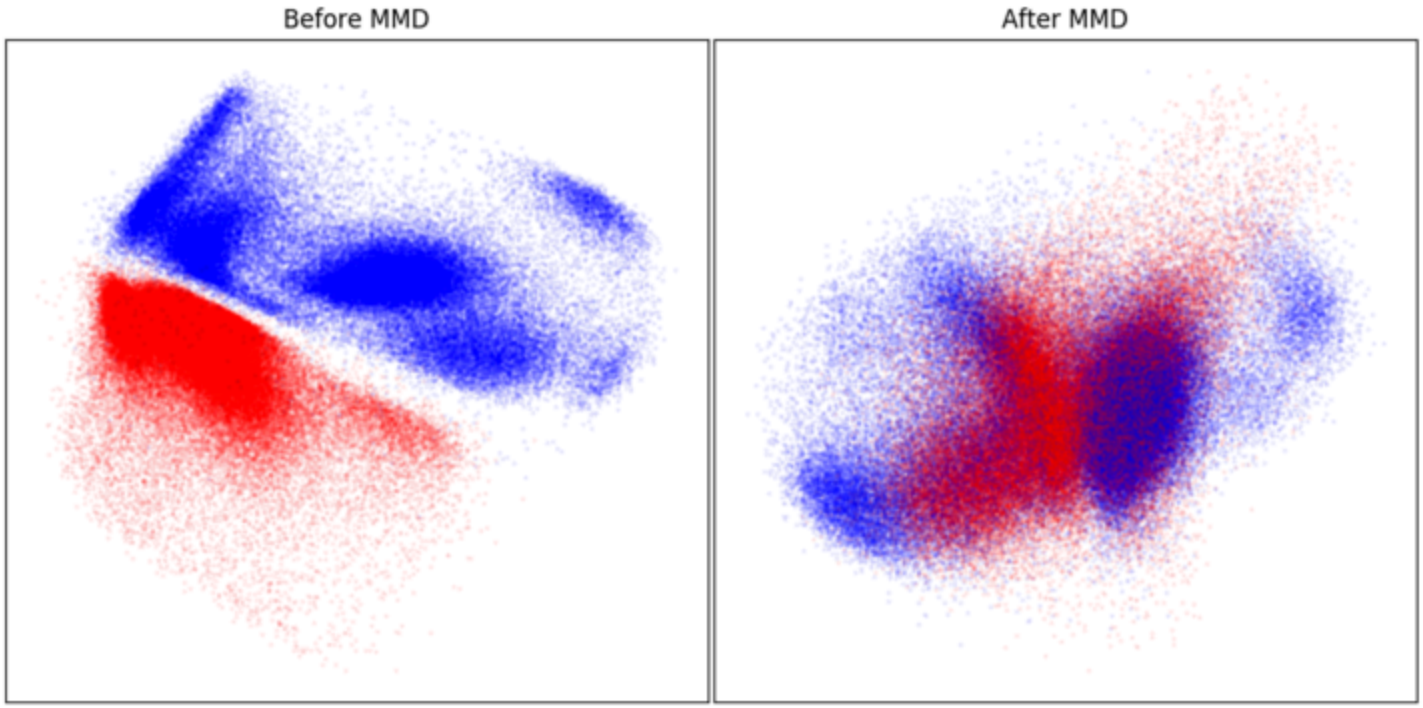
Before MMD
After MMD

High Dimensionality

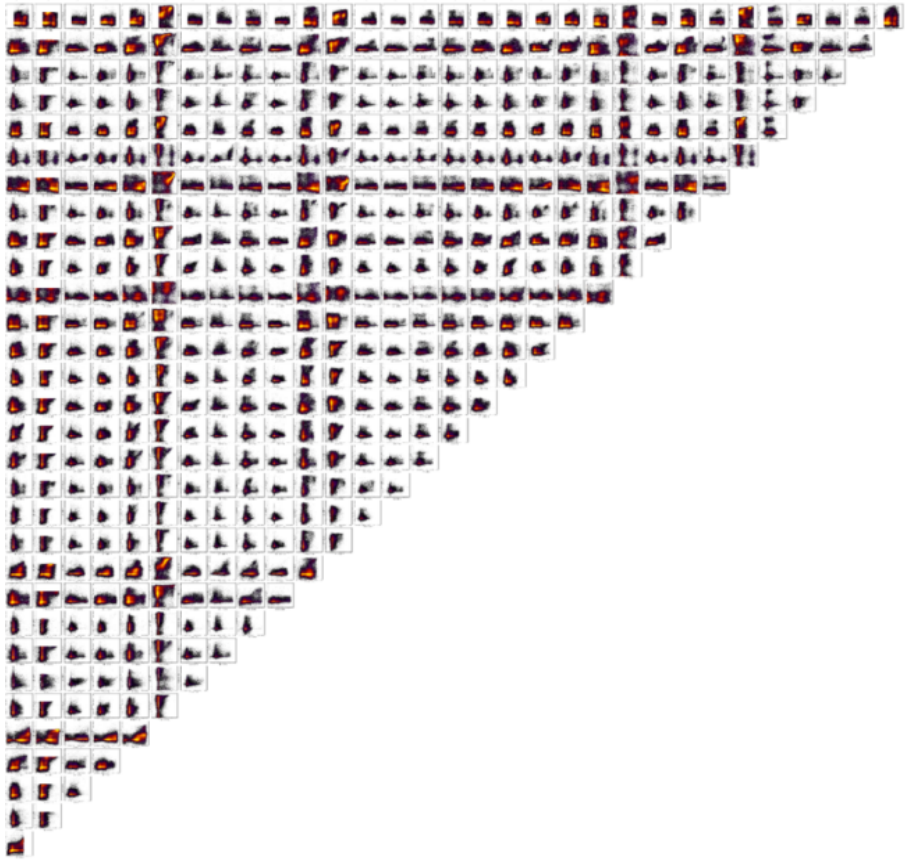

- Systematic differences between samples due to machine calibration, ambient environmental effects
- Variation that is uninteresting to examine and confounds biological variation
- Renders samples incomparable

Latent structure in high dimensional data

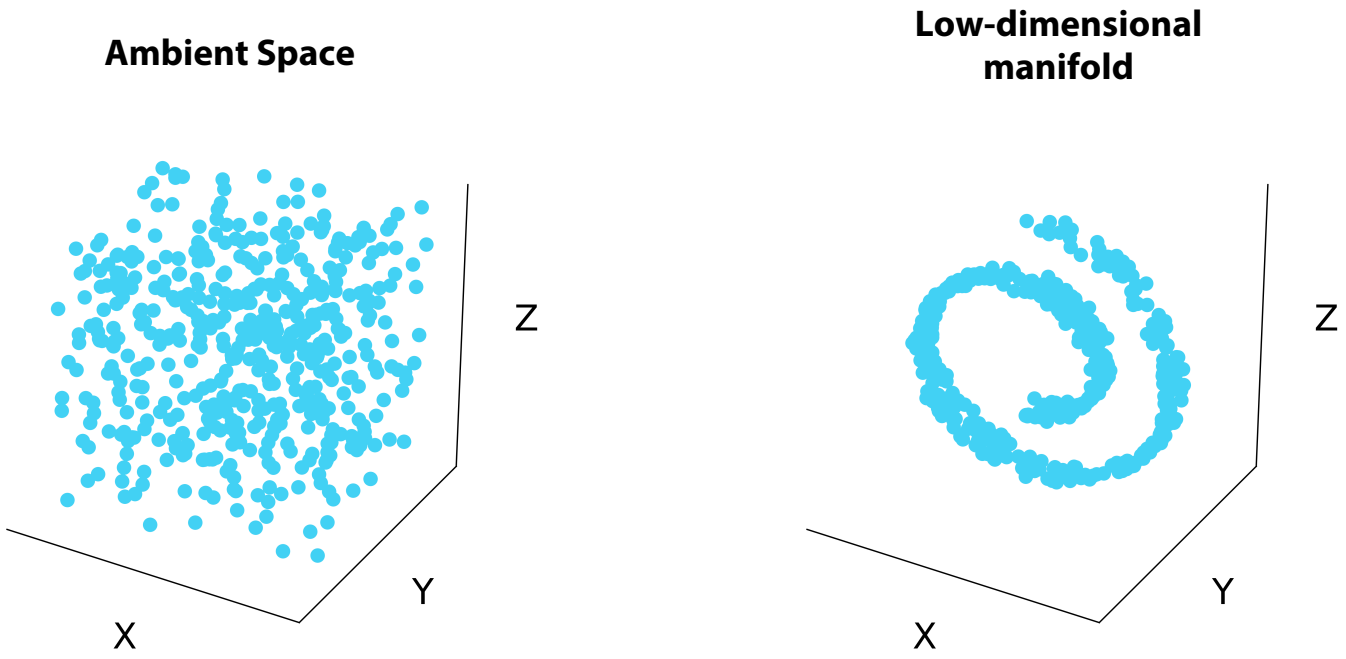

Gene-gene Relationships

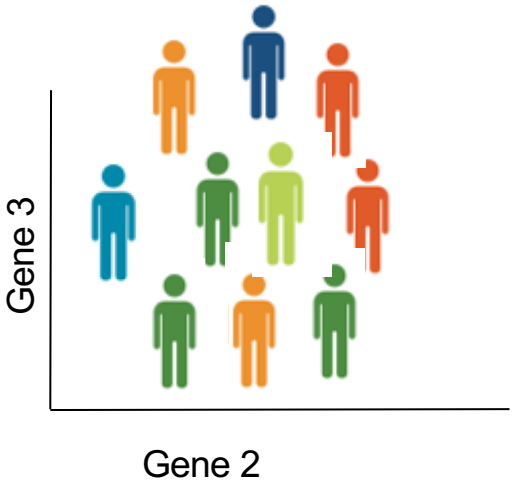

Relationship between features?

Non-linear Relationships

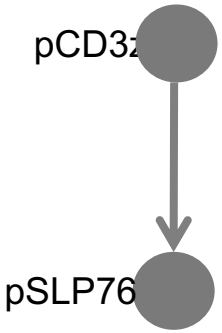

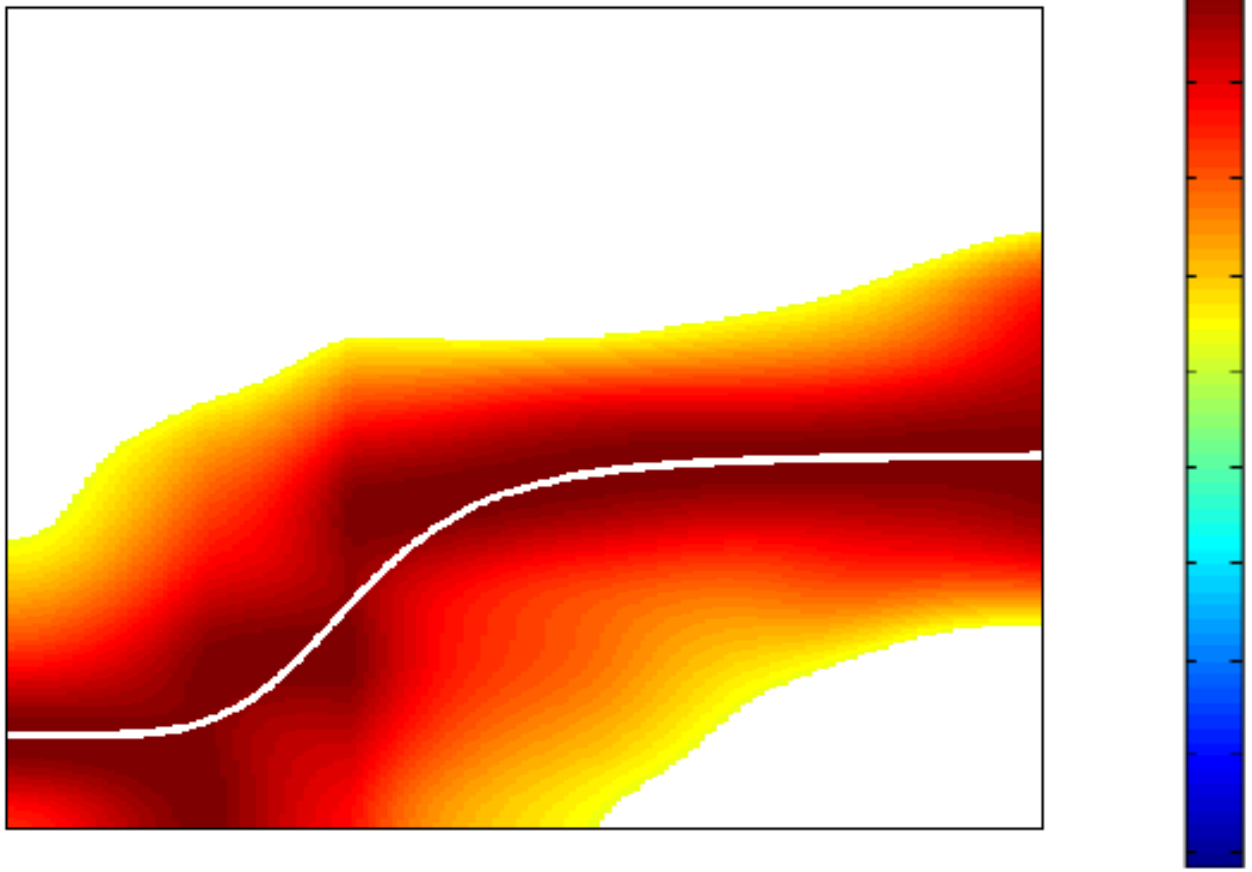

Mutual Information

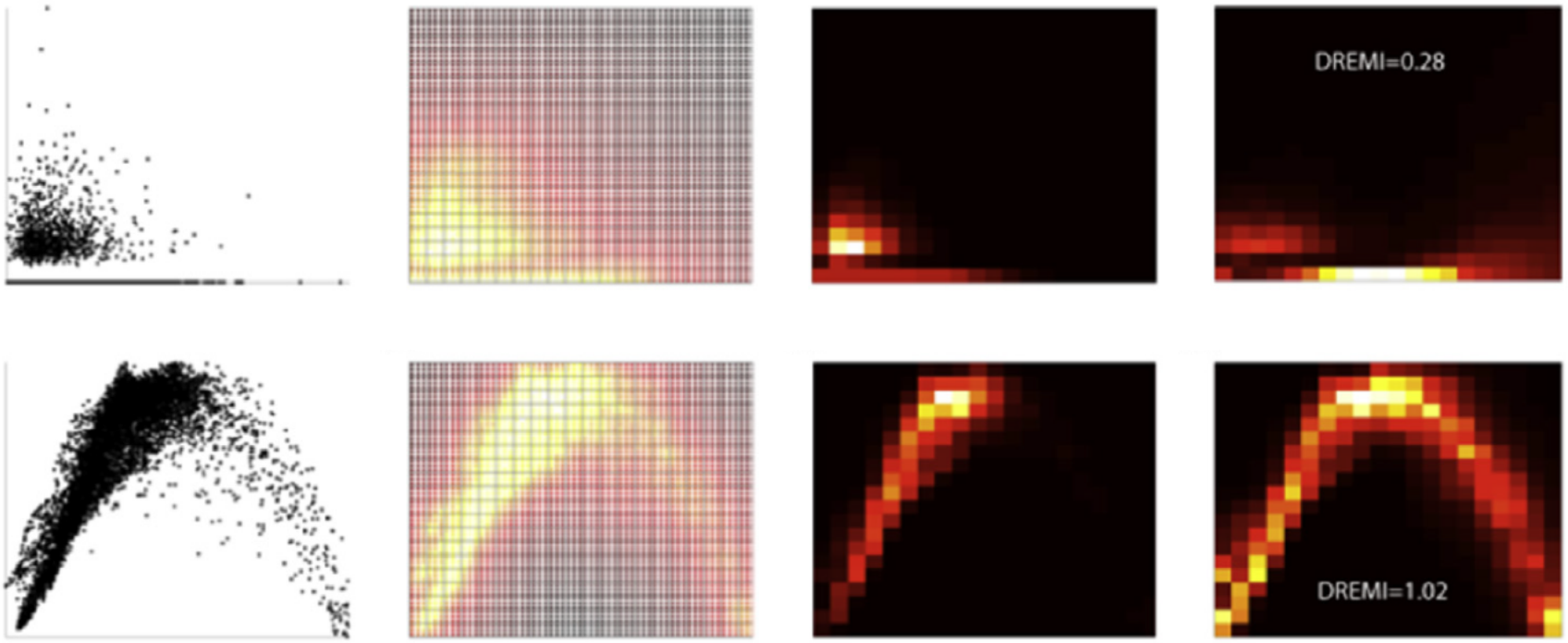

Embedding reveals structure

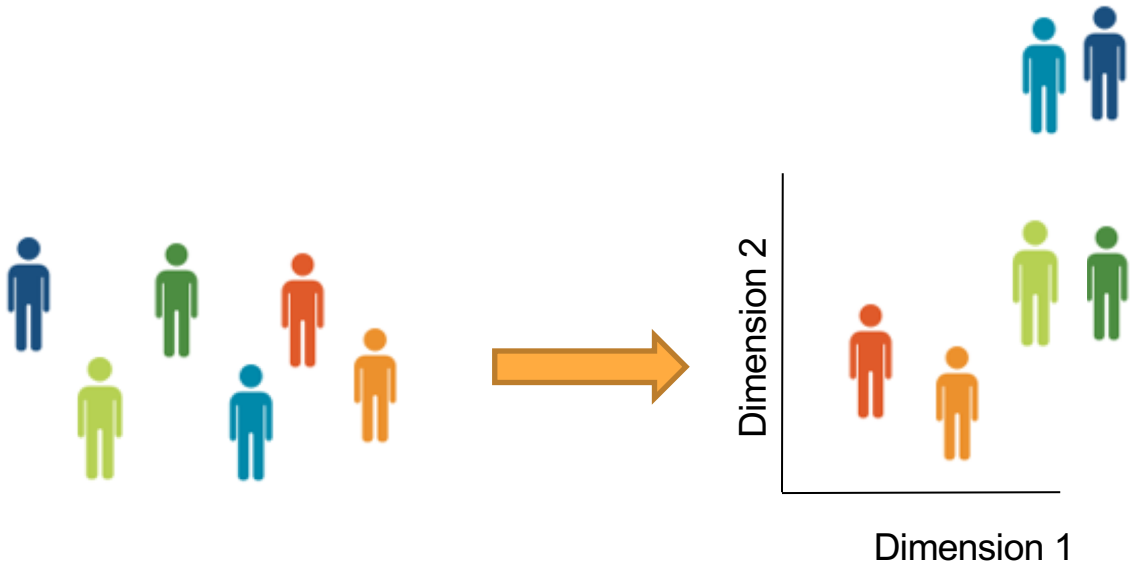

Use high dimensional features and high throughput to understand shape of data

Cluster structure

Excellent Responders

Fair Responders

Poor responders

Retinal Bipolar Cells

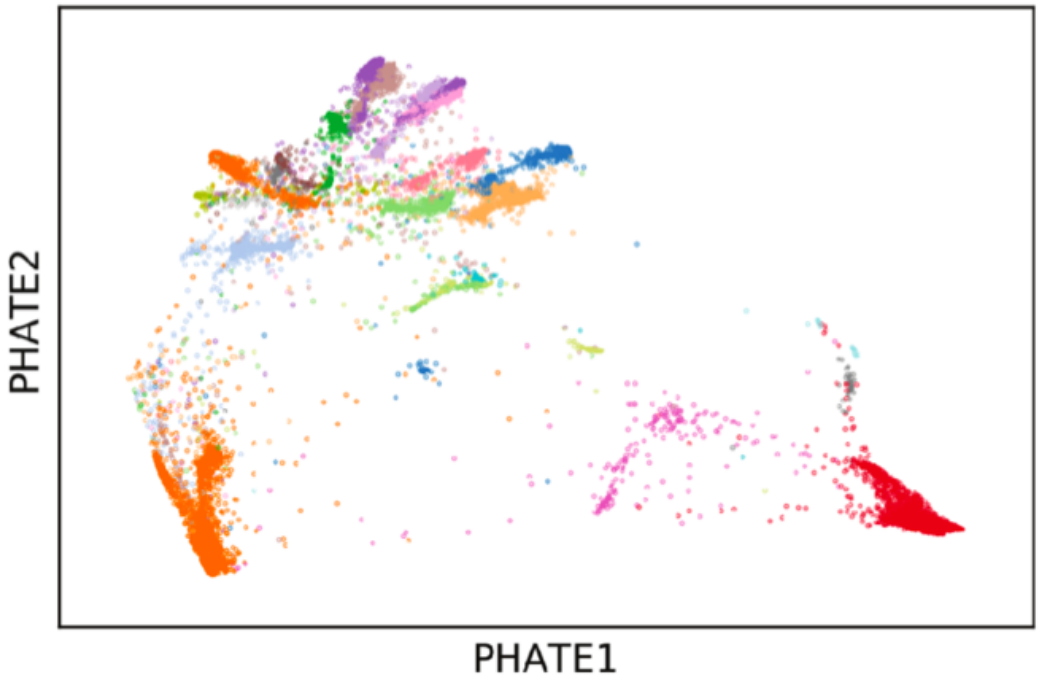

Progression continuum

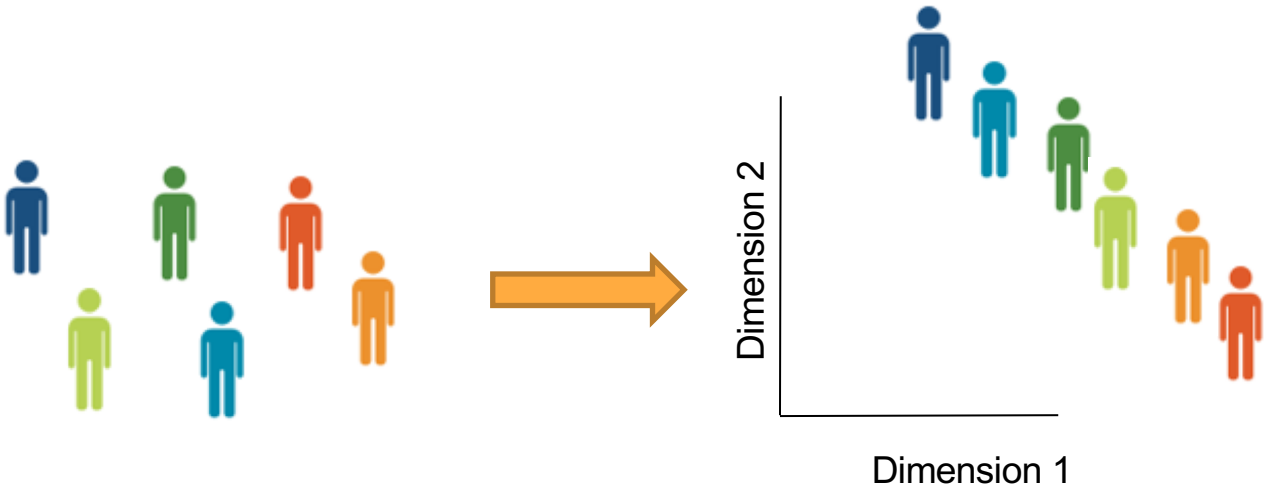

Use high dimensional features and high throughput to understand shape of data

Progressions

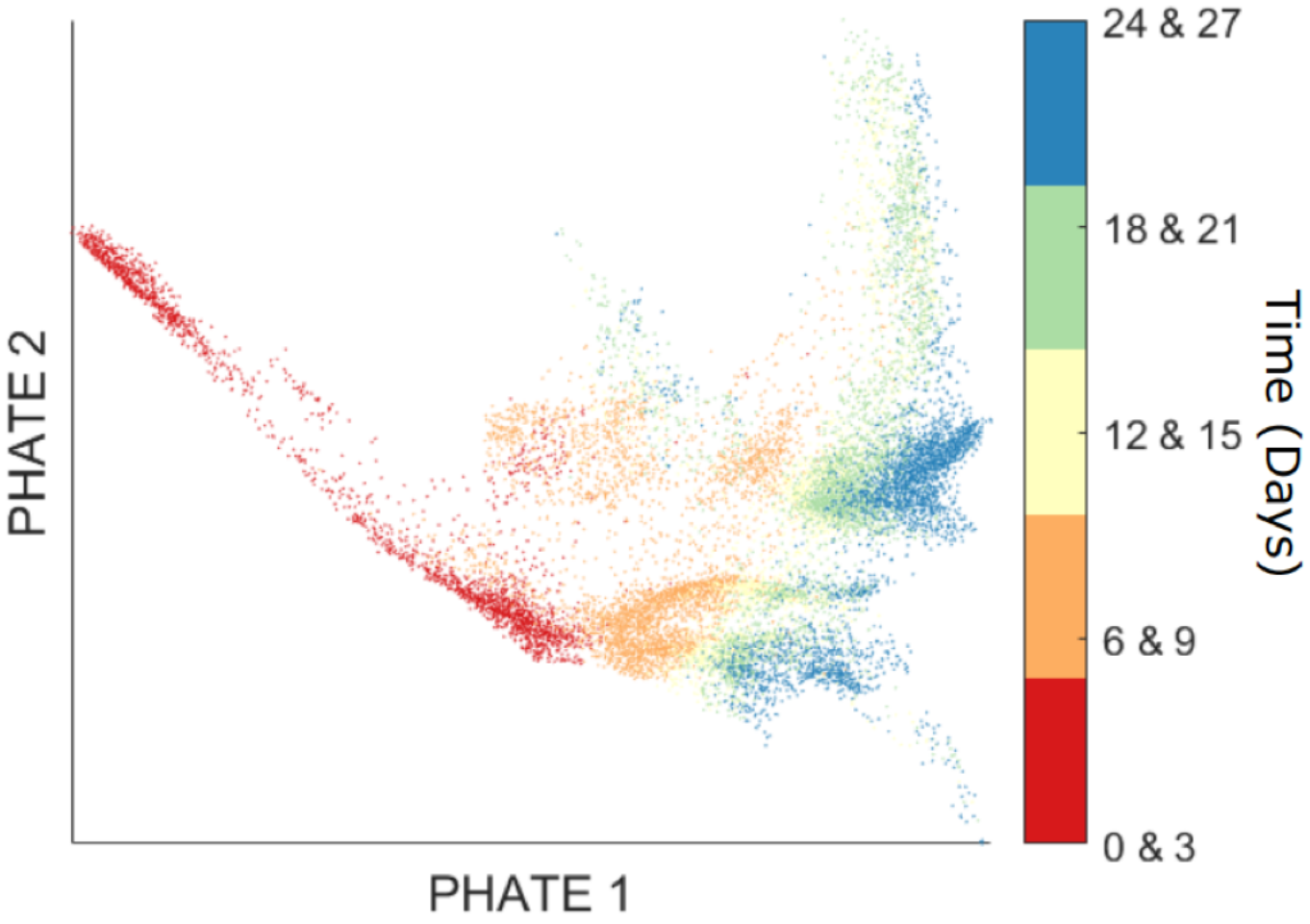

Manifold Learning

Cells are sampled from an underlying manifold

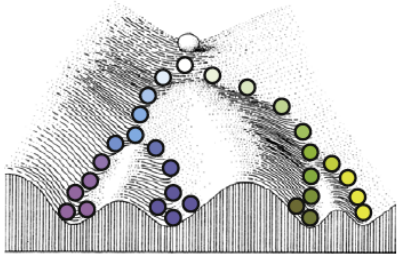

Each cell is represented by a vector of gene expression

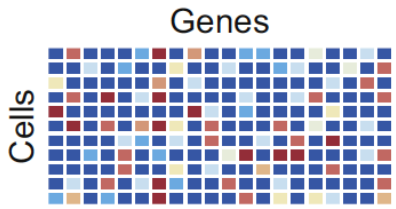

Neighborhood structure of the observations is identfied

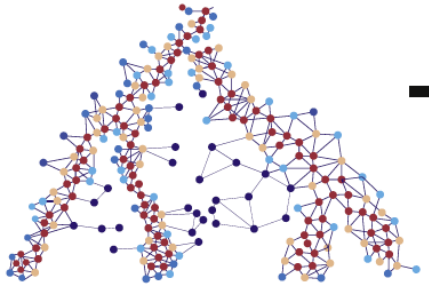

The latent manifold is learned from the data

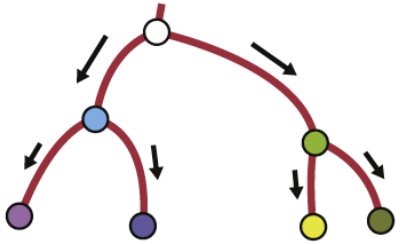

Understanding the shape of data

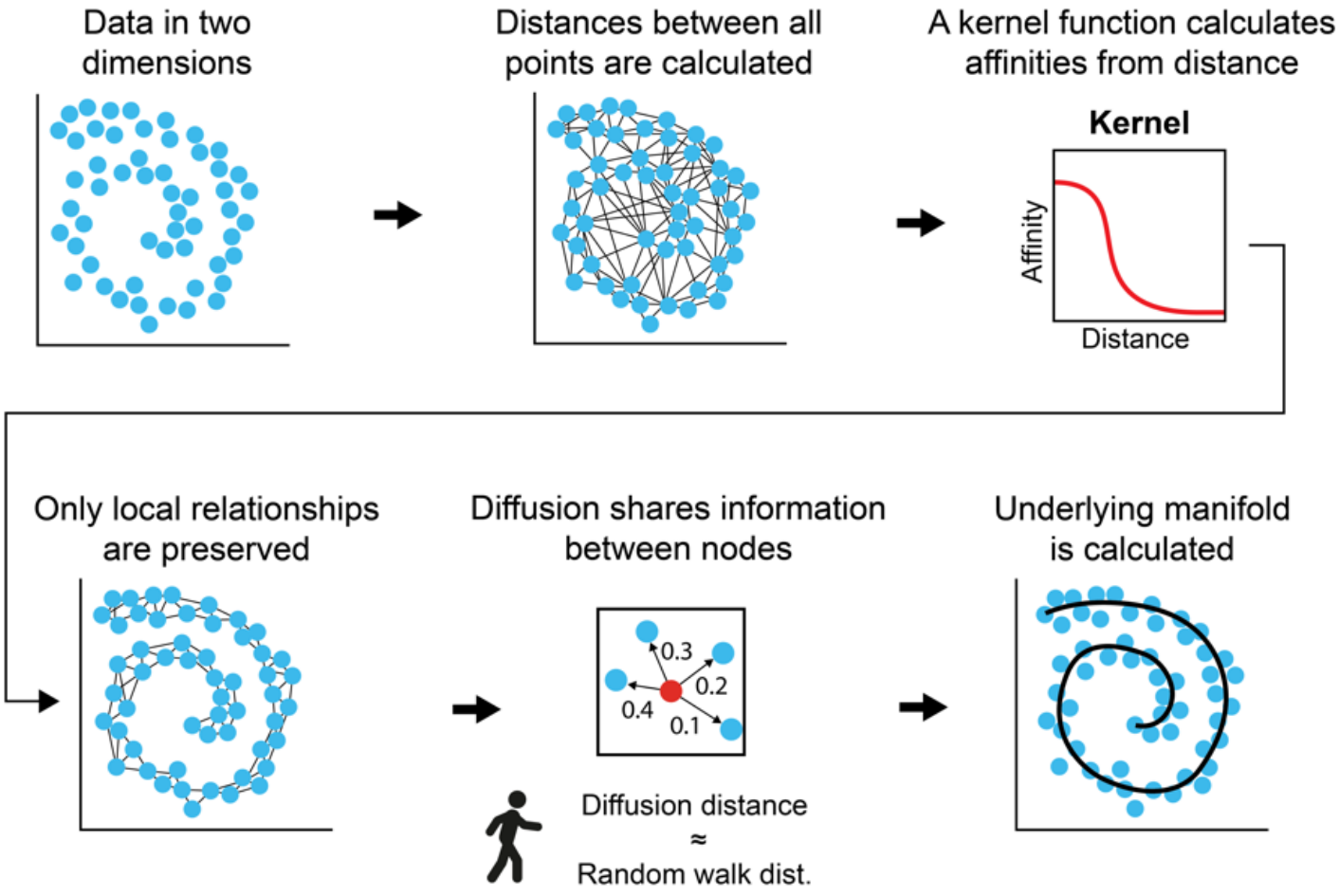

Analysis Tasks

Vizualization

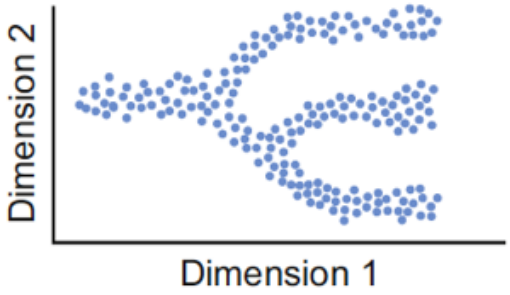

Clustering

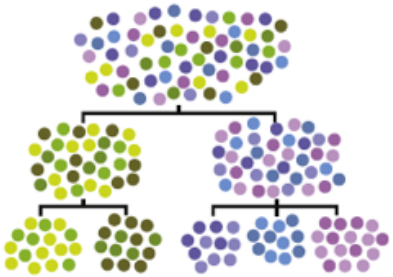

Denoising

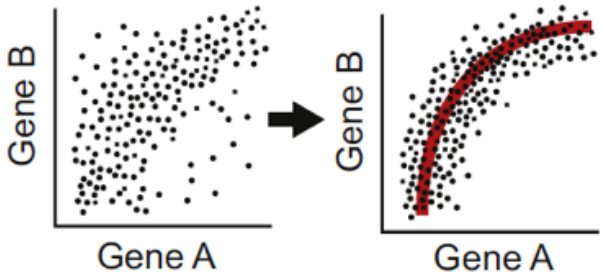

Pseudotime analysis

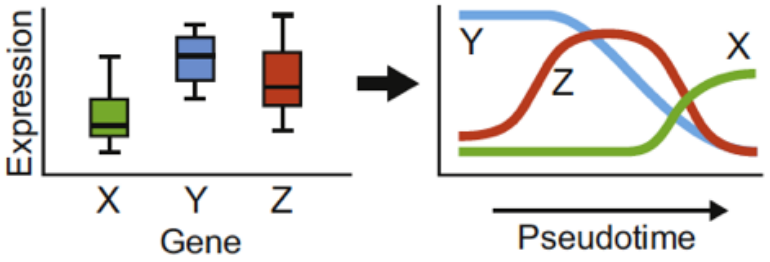

Preprocessing single-cell data

Review

OPEN ACCESS

molecular systems biology

Current best practices in single-cell RNA-seq analysis: a tutorial

Malte D Luecken[1] & Fabian J Theis[1,2,*]

Abstract

Single-cell RNA-seq has enabled gene expression to be studied at an unprecedented resolution. The promise of this technology is attracting a growing user base for single-cell analysis methods. As more analysis tools are becoming available, it is becoming increasingly difficult to navigate this landscape and produce an up-to-date workflow to analyse one's data. Here, we detail the steps of a typical single-cell RNA-seq analysis, including pre-processing (quality control, normalization, data correction, feature selection, and dimensionality reduction) and cell- and gene-level downstream analysis. We formulate current best-practice recommendations for these steps based on independent comparison studies. We have integrated these best-practice recommendations into a workflow, which we apply to a public dataset to further illustrate how these steps work in practice. Our documented case study can be found at https://www.github.com/theislab/single-cell-tutorial. This review will serve as a workflow tutorial for new entrants into the field, and help established users update their analysis pipelines.

Keywords analysis pipeline development; computational biology; data analysis tutorial; single-cell RNA-seq

DOI 10.15252/msb.20188746 | Received 16 November 2018 | Revised 15 March 2019 | Accepted 3 April 2019

Mol Syst Biol. (2019) 15: e8746

Introduction

In recent years, single-cell RNA sequencing (scRNA-seq) has significantly advanced our knowledge of biological systems. We have been able to both study the cellular heterogeneity of zebrafish, frogs outline current best practices to lay a foundation for future analysis standardization.

The challenges to standardization include the growing number of analysis methods (385 tools as of 7 March 2019) and exploding dataset sizes (Angerer *et al*, 2017; Zappia *et al*, 2018). We are continuously finding new ways to use the data at our disposal. For example, it has recently become possible to predict cell fates in differentiation (La Manno *et al*, 2018). While the continuous improvement of analysis tools is beneficial for generating new scientific insight, it complicates standardization.

Further challenges for standardization lie in technical aspects. Analysis tools for scRNA-seq data are written in a variety of programming languages—most prominently R and Python (Zappia *et al*, 2018). Although cross-environment support is growing (preprint: Scholz *et al*, 2018), the choice of programming language is often also a choice between analysis tools. Popular platforms such as Seurat (Butler *et al*, 2018), Scater (McCarthy *et al*, 2017), or Scanpy (Wolf *et al*, 2018) provide integrated environments to develop pipelines and contain large analysis toolboxes. However, out of necessity these platforms limit themselves to tools developed in their respective programming languages. By extension, language restrictions also hold true for currently available scRNA-seq analysis tutorials, many of which revolve around the above platforms (R and bioconductor tools: https://github.com/drisso/bioc2016singlecell and https://hemberg-lab.github.io/scRNA.seq.course/; Lun *et al*, 2016b; Seurat: https://satijalab.org/seurat/get_started.html; Scanpy: https://scanpy.readthedocs.io/en/stable/tutorials.html).

Considering the above-mentioned challenges, instead of targeting a standardized analysis pipeline, we outline current best practices and common tools independent of programming language. We guide the reader through the various steps of a scRNA-seq analysis pipeline (Fig 1), present current best practices, and discuss analysis

https://doi.org/10.15252/msb.20188746

Standard Single-Cell RNA-seq Workflow

1. Sequencing and read mapping
2. Quality control and filtering
3. Normalization
4. Data Correction

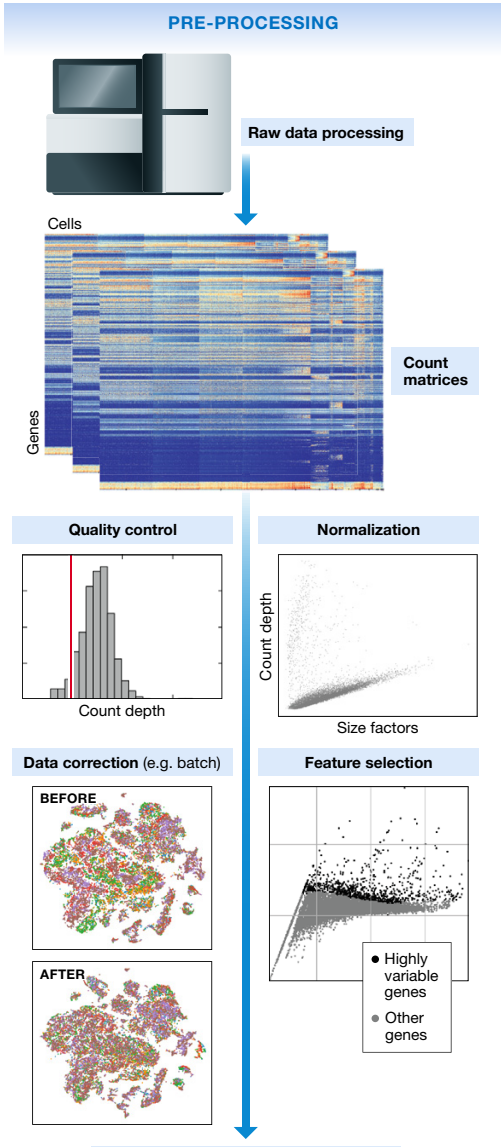

Standard Single-Cell RNA-seq Workflow

1. Sequencing and read mapping
2. Quality control and filtering
3. Normalization
4. Data Correction
5. Dimensionality reduction and visualization

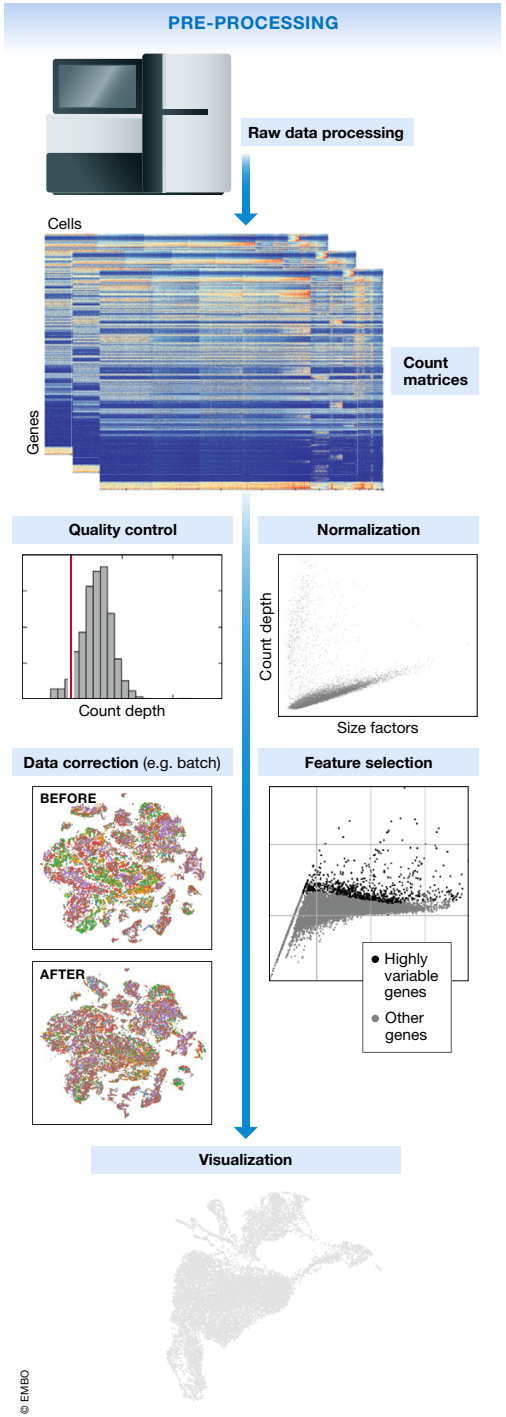

Standard Single-Cell RNA-seq Workflow

1. Sequencing and read mapping
2. Quality control and filtering
3. Normalization
4. Data Correction
5. Dimensionality reduction and visualization
6. Downstream analysis
    1. Clustering
    2. Trajectory inference

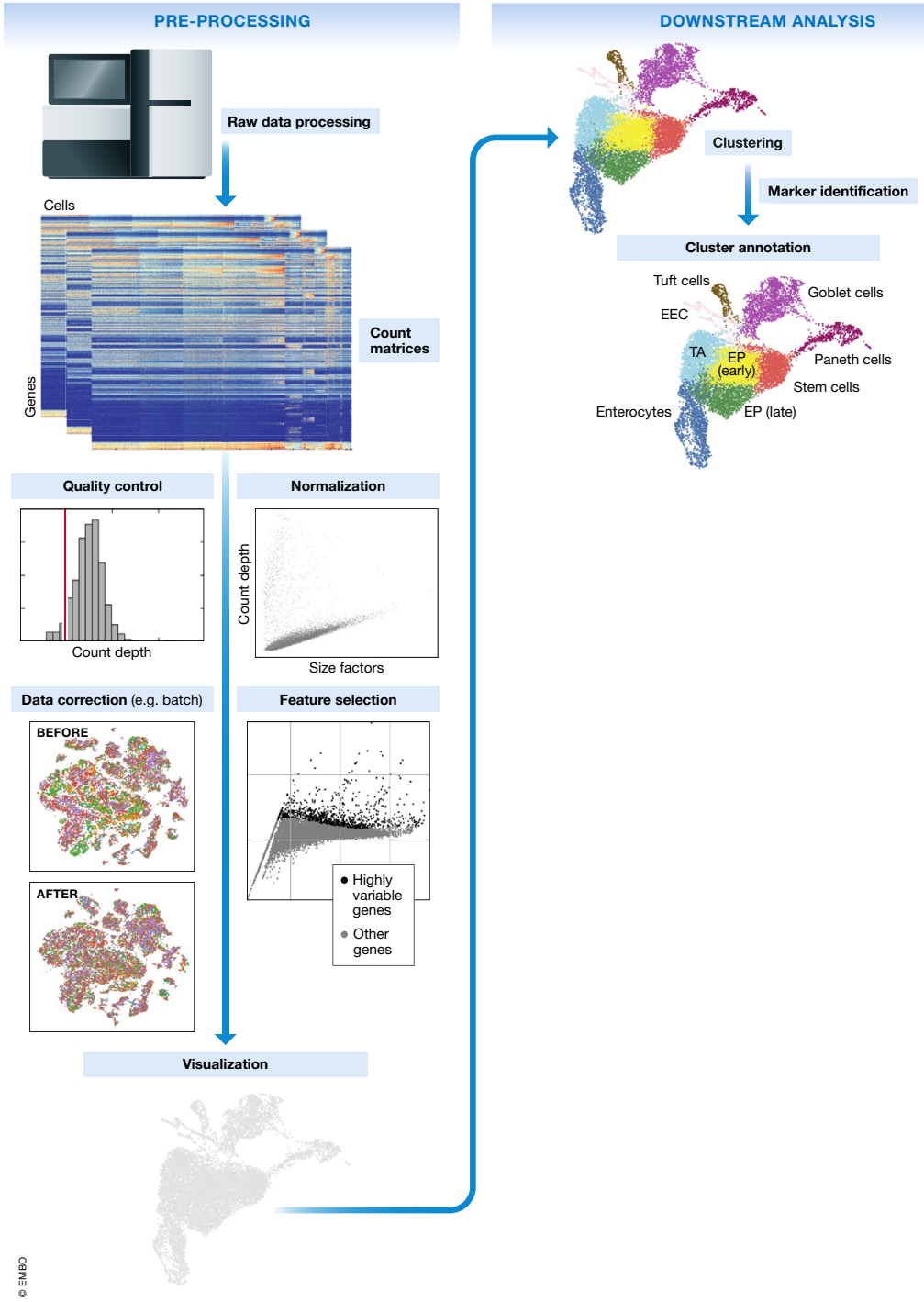

Standard Single-Cell RNA-seq Workflow

1. Sequencing and read mapping
2. Quality control and filtering
3. Normalization
4. Data Correction
5. Dimensionality reduction and visualization
6. Downstream analysis
    1. Clustering
    2. Trajectory inference
    3. Differential expression

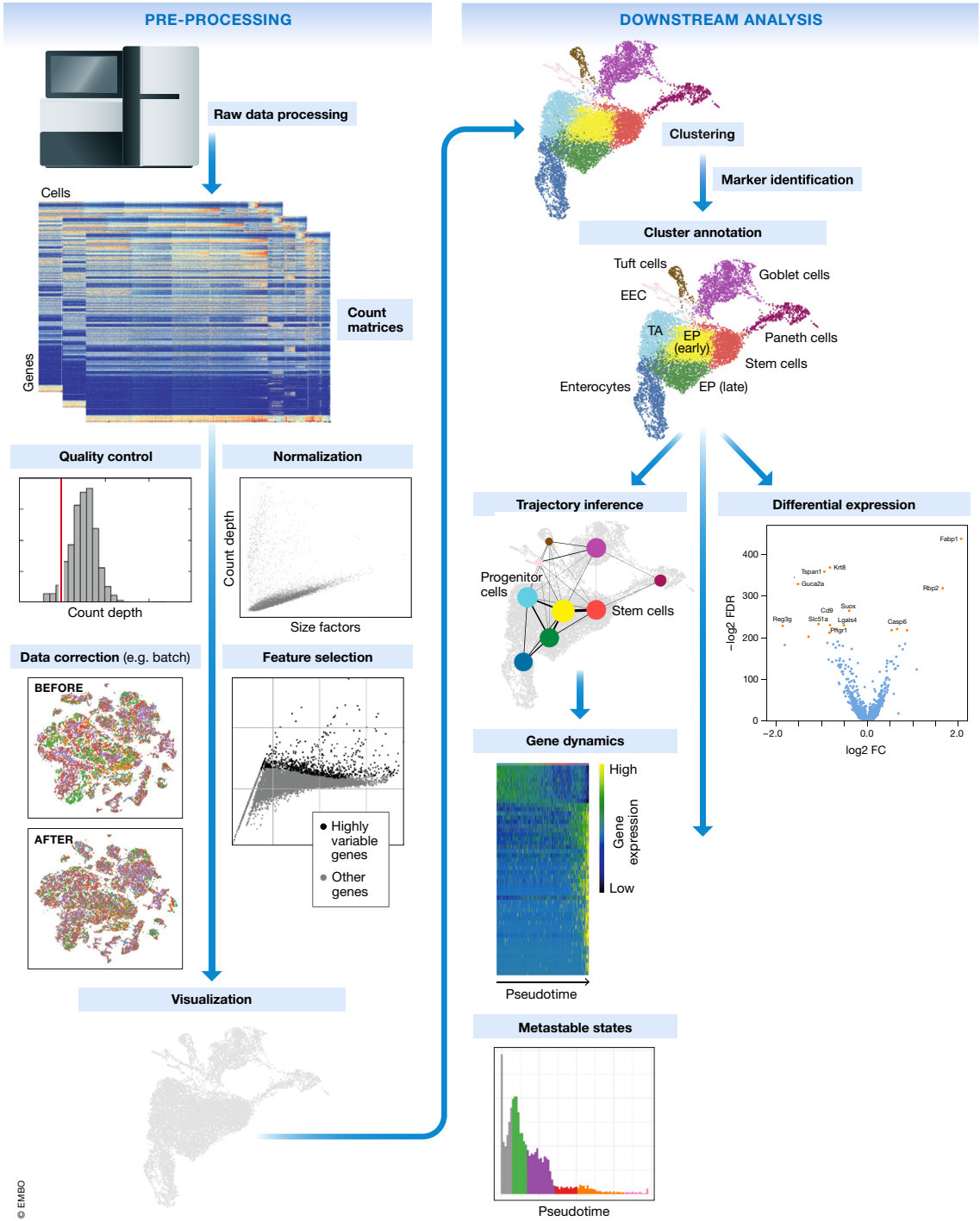

Standard Single-Cell RNA-seq Workflow

1. Sequencing and read mapping
2. Quality control and filtering
3. Normalization
4. Data Correction
5. Dimensionality reduction and visualization
6. Downstream analysis
    1. Clustering
    2. Trajectory inference
    3. Differential expression
7. Comparison of multiple conditions

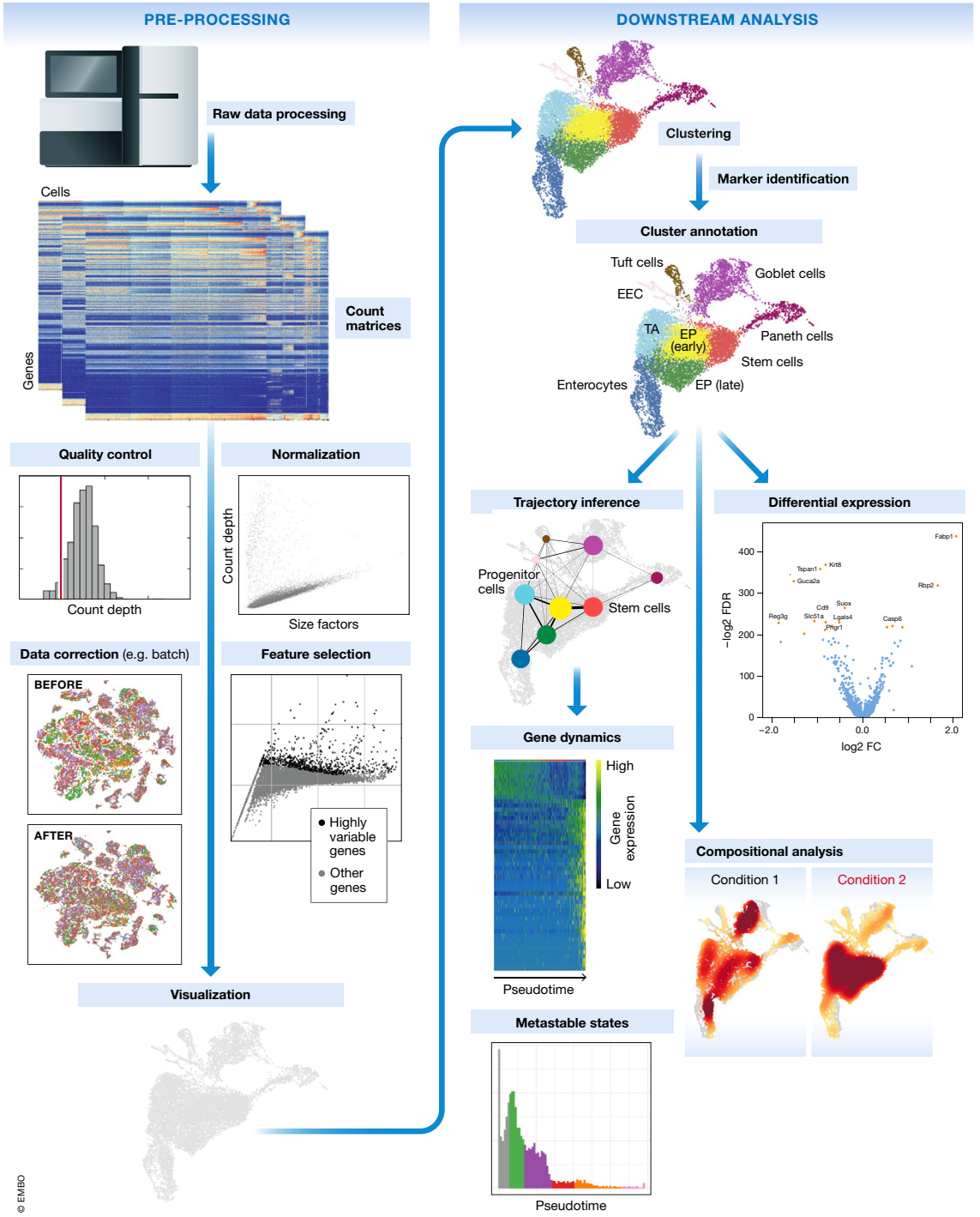

Step 1 - Sequencing & read mapping

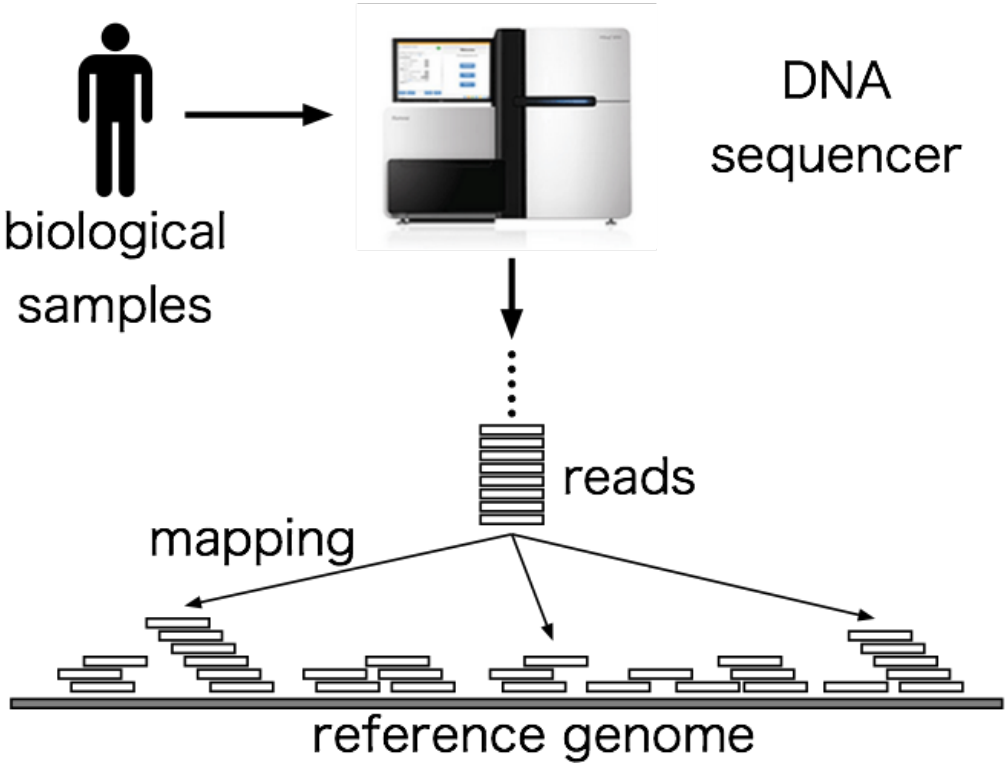

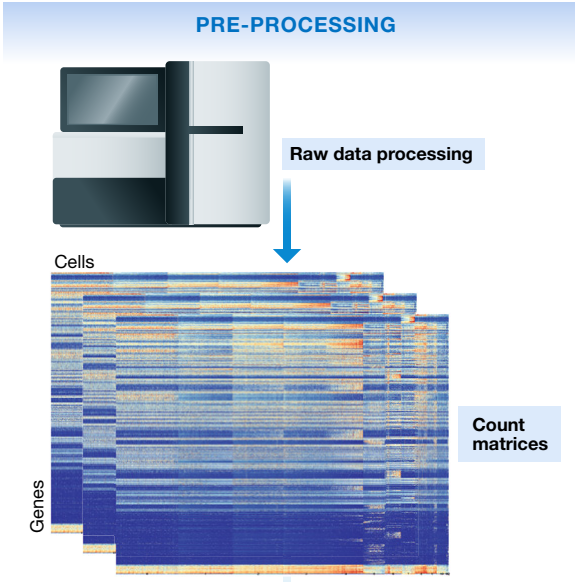

Step 2 – Quality control and filtering

Dying cells

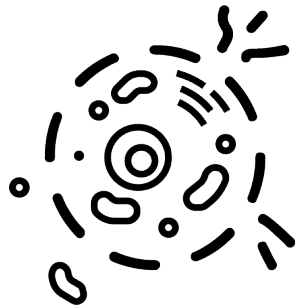

Multiplets

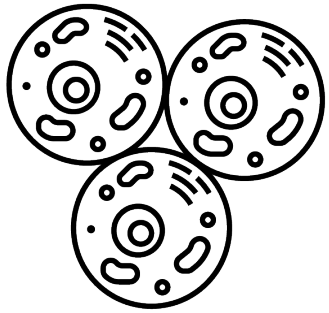

Empty Droplets

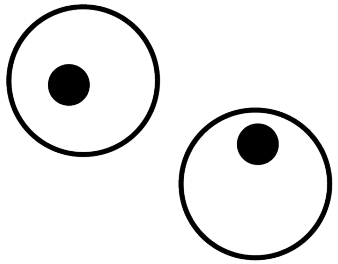

What could we look at to discriminate between dying cells, multiplets, or empty droplets and healthy single cells?

Top

Step 2 – Quality control and filtering

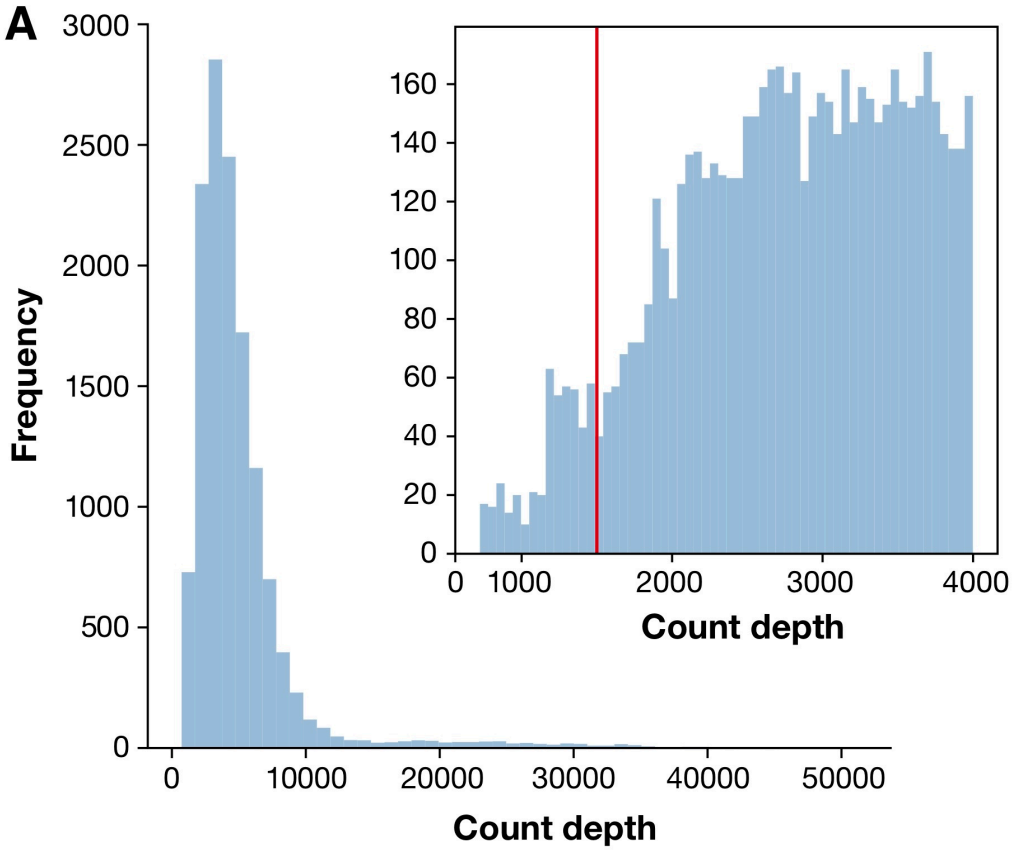

Step 2 – Quality control and filtering

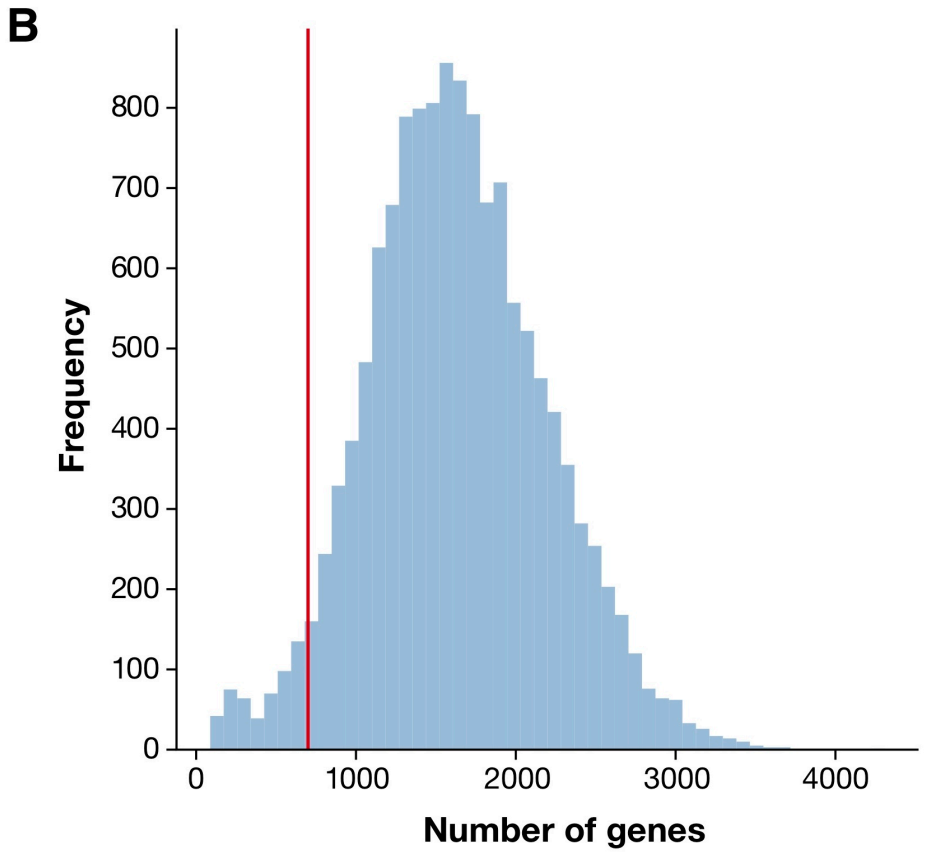

Step 2 – Quality control and filtering

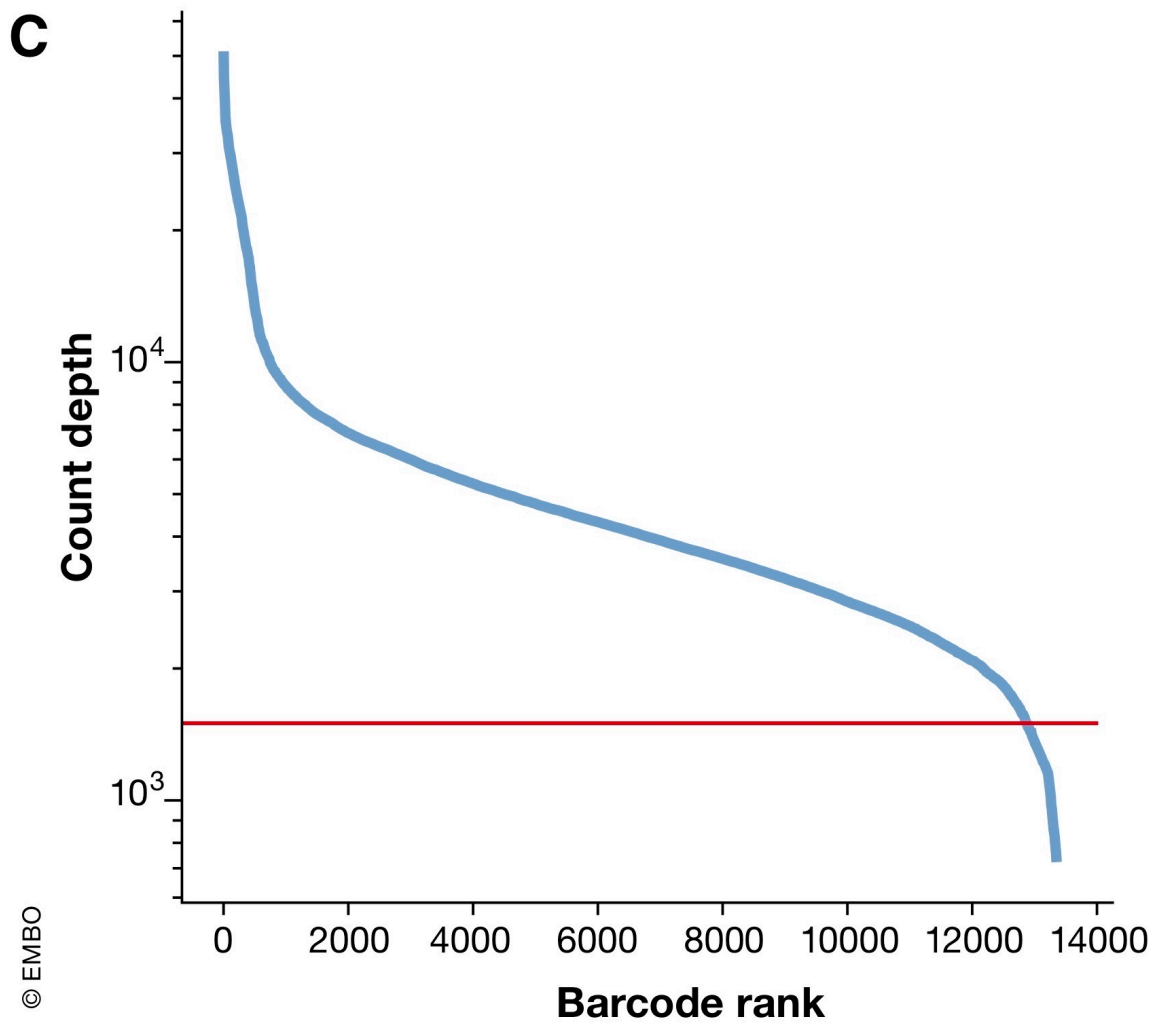

Building Counts Matrix → QC & Filtering → Normalization → Visualization → Analysis

Step 2 – Quality control and filtering

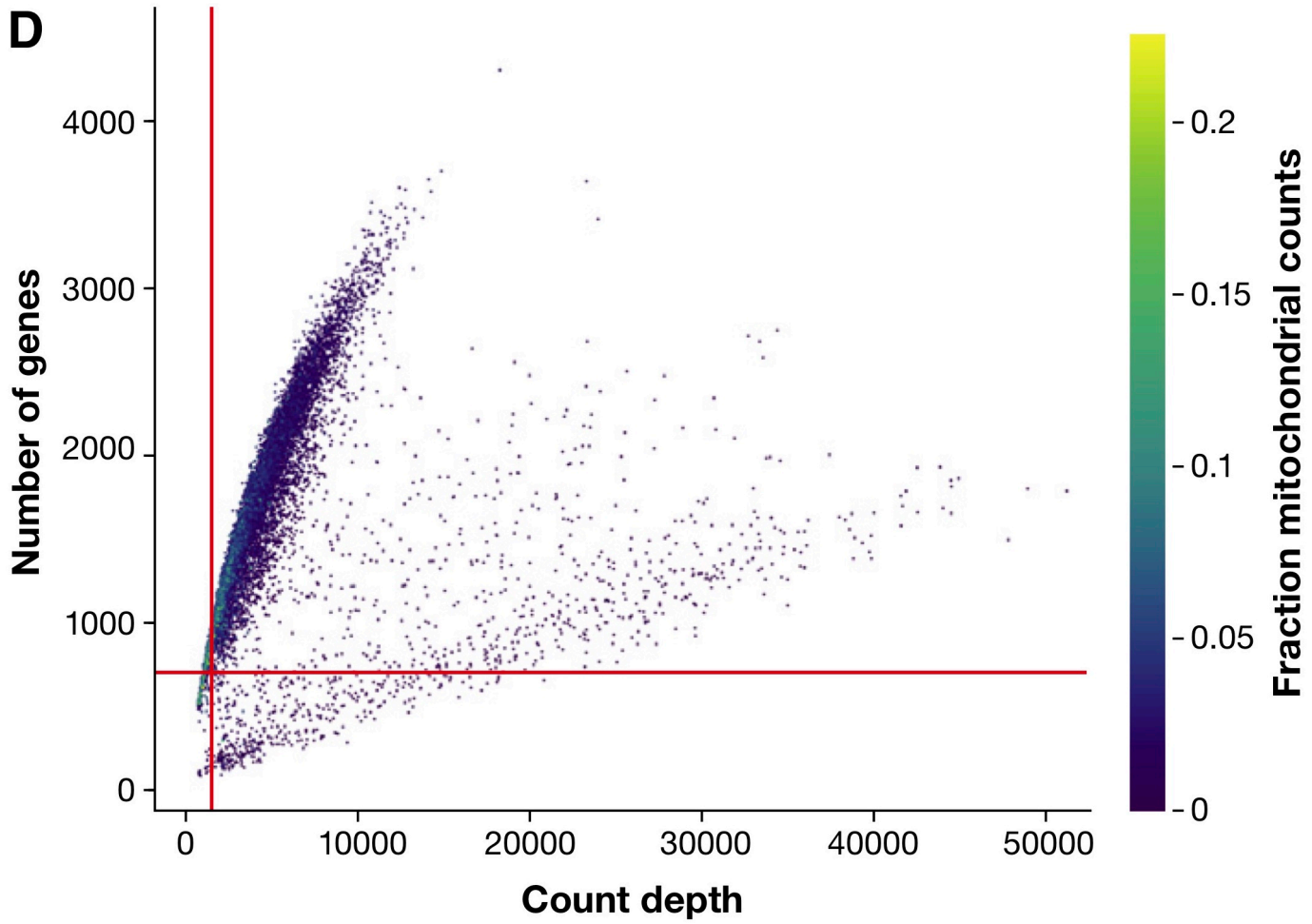

Step 3 - Normalization

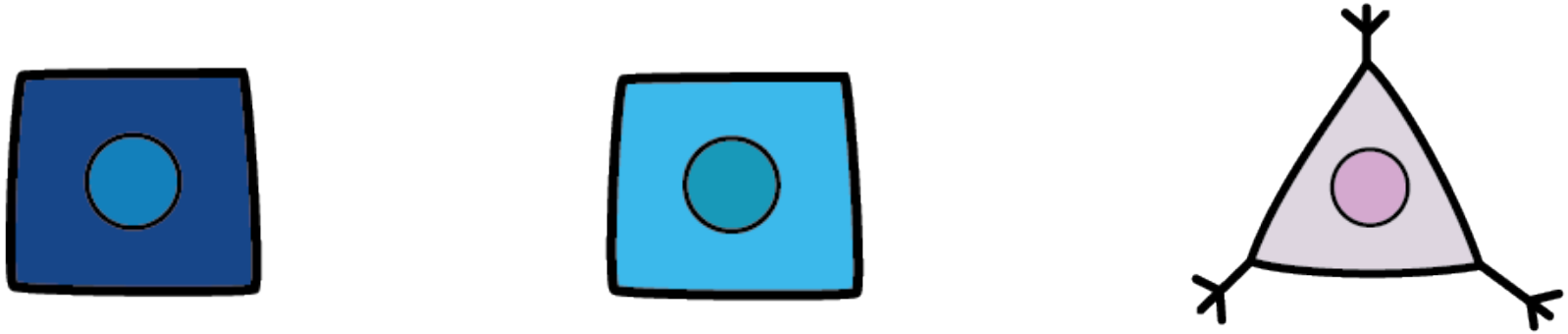

If we only have gene expression, how can we determine which cells are similar?

Step 3 - Normalization

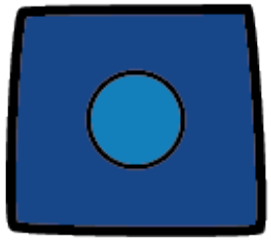

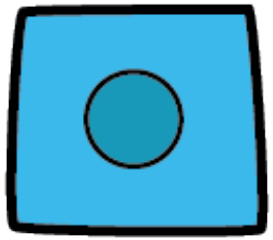

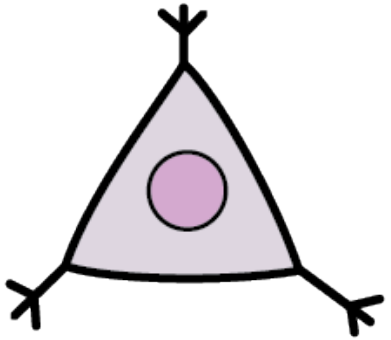

10% Capture Efficiency

Gene	Cell A
X	10
Y	20
Z	70

Step 3 - Normalization

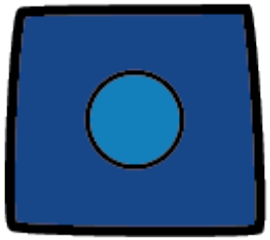

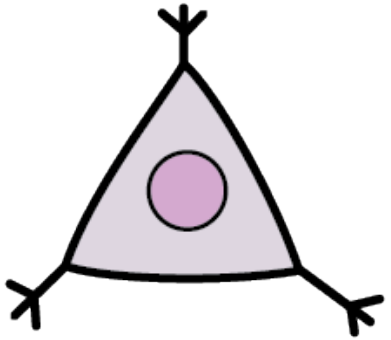

10% Capture Efficiency

Gene	Cell A
X	10
Y	20
Z	70

20% CE

Gene	Cell B
X	20
Y	40
Z	140

Step 3 - Normalization

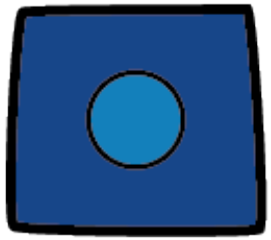

10% Capture Efficiency

Gene	Cell A
X	10
Y	20
Z	70

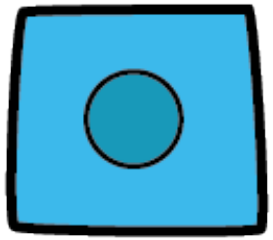

20% CE

Gene	Cell B
X	20
Y	40
Z	140

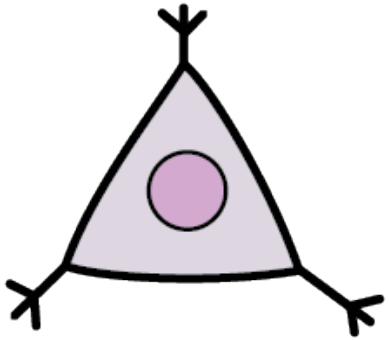

20% CE

Gene	Cell C
X	20
Y	0
Z	80

Step 3 - Normalization

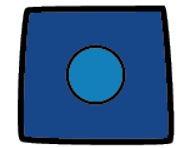

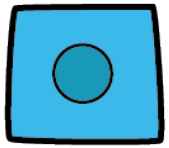

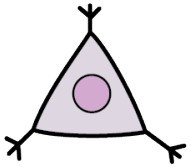

Raw counts

	X	Y	Z
A	10	20	70
B	20	40	140
C	20	0	80

Step 3 - Normalization

Raw counts

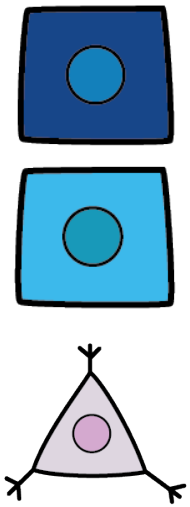

	X	Y	Z
A	10	20	70
B	20	40	140
C	20	0	80

$$\text{dist(A,B)} = \sqrt{(x_A - x_B)^2 + (y_a - y_b)^2 + (z_a - z_b)^2}$$

Step 3 - Normalization

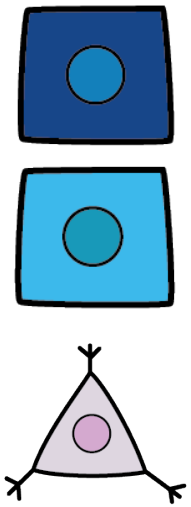

Raw counts

	X	Y	Z
A	10	20	70
B	20	40	140
C	20	0	80

Pairwise distances

dist(A,B) = 71.4

$$\text{dist(A,B)} = \sqrt{(x_A - x_B)^2 + (y_a - y_b)^2 + (z_a - z_b)^2}$$

Step 3 - Normalization

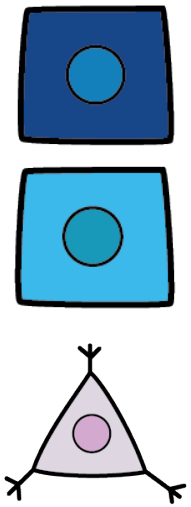

Raw counts

	X	Y	Z
A	10	20	70
B	20	40	140
C	20	0	80

Pairwise distances

dist(A,B) = 71.4

dist(A,C) = 24.5

dist(B,C) = 67.1

$$\text{dist(A,B)} = \sqrt{(x_A - x_B)^2 + (y_a - y_b)^2 + (z_a - z_b)^2}$$

Step 3 - Normalization

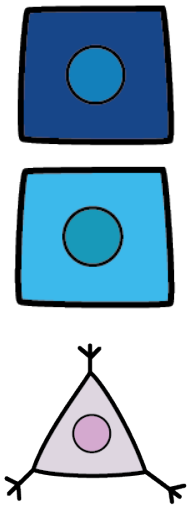

Raw counts

	X	Y	Z	Library Size
A	10	20	70	100
B	20	40	140	200
C	20	0	80	100

Pairwise distances

dist(A,B) = 71.4

dist(A,C) = 24.5

dist(B,C) = 67.1

$$\text{dist(A,B)} = \sqrt{(x_A - x_B)^2 + (y_a - y_b)^2 + (z_a - z_b)^2}$$

Step 3 - Normalization

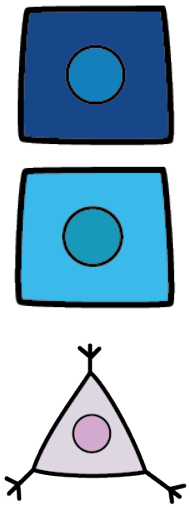

Normalized counts

	X	Y	Z	Library Size
A	0.1	0.2	0.7	100
B	0.1	0.2	0.7	200
C	0.2	0	0.8	100

Pairwise distances

dist(A,B) = 71.4

dist(A,C) = 24.5

dist(B,C) = 67.1

$$\text{dist(A,B)} = \sqrt{(x_A - x_B)^2 + (y_a - y_b)^2 + (z_a - z_b)^2}$$

Step 3 - Normalization

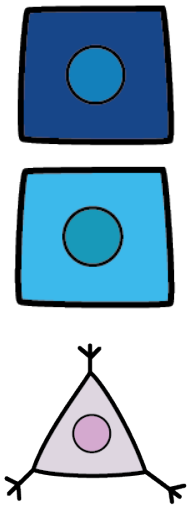

Normalized counts

	X	Y	Z	Library Size
A	0.1	0.2	0.7	100
B	0.1	0.2	0.7	200
C	0.2	0	0.8	100

Pairwise distances

dist(A,B) = 0

dist(A,C) = 0.25

dist(B,C) = 0.25

$$\text{dist(A,B)} = \sqrt{(x_A - x_B)^2 + (y_a - y_b)^2 + (z_a - z_b)^2}$$

More complex normalization approaches exist

Fig. 3

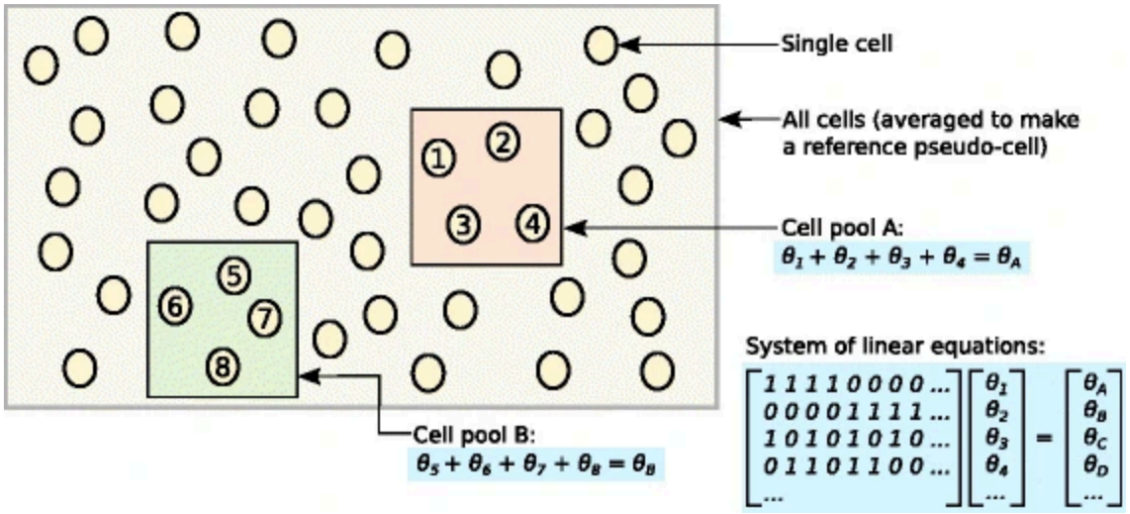

Schematic of the deconvolution method. All cells in the data set are averaged to make a reference pseudo-cell. Expression values for cells in pool A are summed together and normalized against the reference to yield a pool-based size factor θ_A. This is equal to the sum of the cell-based factors θ_j for cells j=1–4 and can be used to formulate a linear equation. (For simplicity, the t_j term is assumed to be unity here.) Repeating this for multiple pools (e.g., pool B) leads to the construction of a linear system that can be solved to estimate θ_j for each cell j

https://doi.org/10.1186/s13059-016-0947-7

Step 3.5 – Transformation / Scaling

Normalized counts

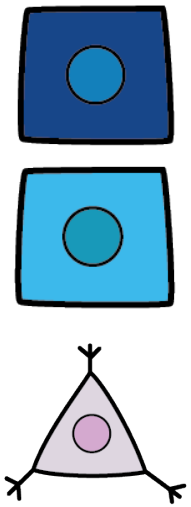

	X	Y	Z
A	0.1	0.2	0.7
B	0.1	0.2	0.7
C	0.2	0	0.8

What if this is a housekeeping gene?

What if this is a transcription factor?

Step 3.5 – Transformation / Scaling

sqrt(normalized counts)

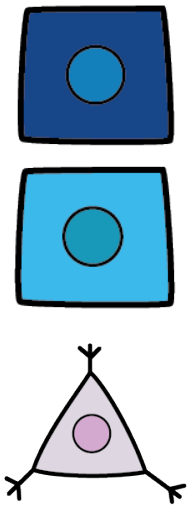

	X	Y	Z
A	0.32	0.45	0.84
B	0.32	0.45	0.89
C	0.2	0	0.89

What if this is a housekeeping gene?

What if this is a transcription factor?

What kind of transformations, other than square-root, could we apply to single cell data?

Top

Step 5 – Dimensionality reduction and visualization

Selecting highly variable genes (HVGs):

- Calculate log10 mean expression and variance
- Fit a loess curve
- Standardize variance to mean 0 std 1
- Take the top 2000 HVGs

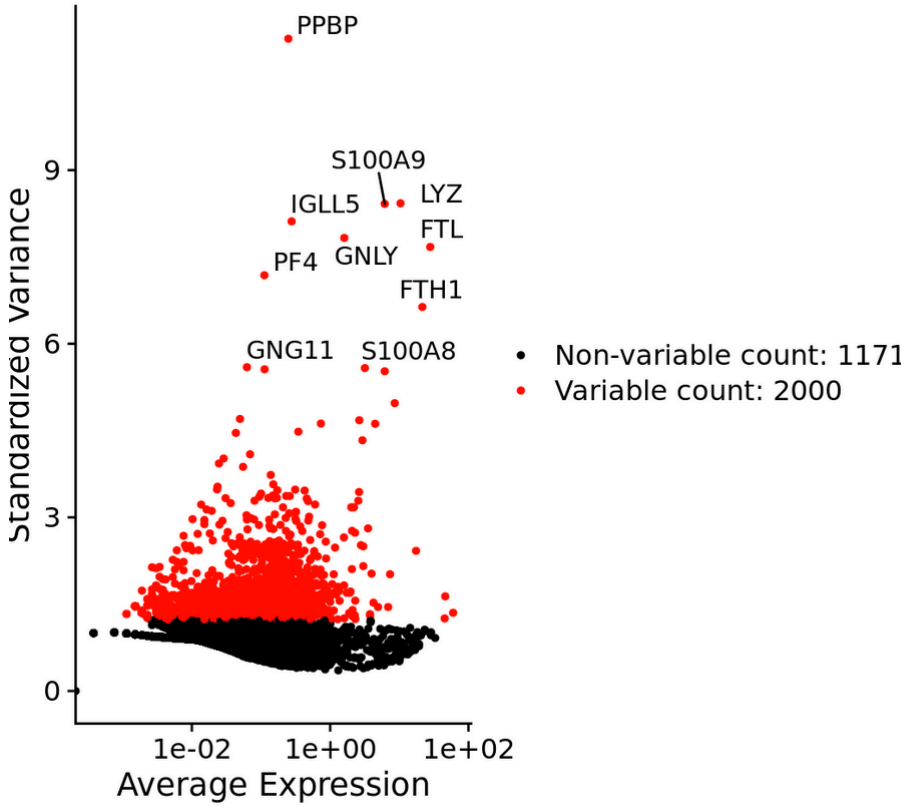

Building Counts Matrix → QC & Filtering → Normalization → Visualization → Analysis

https://satijalab.org/seurat/v3.1/pbmc3k_tutorial.htm

Standard Single-Cell RNA-seq Workflow

1. Sequencing and read mapping
2. Quality control and filtering
3. Normalization
4. Data Correction
5. Dimensionality reduction and visualization
6. Downstream analysis
    1. Clustering
    2. Trajectory inference
    3. Differential expression
7. Comparison of multiple conditions

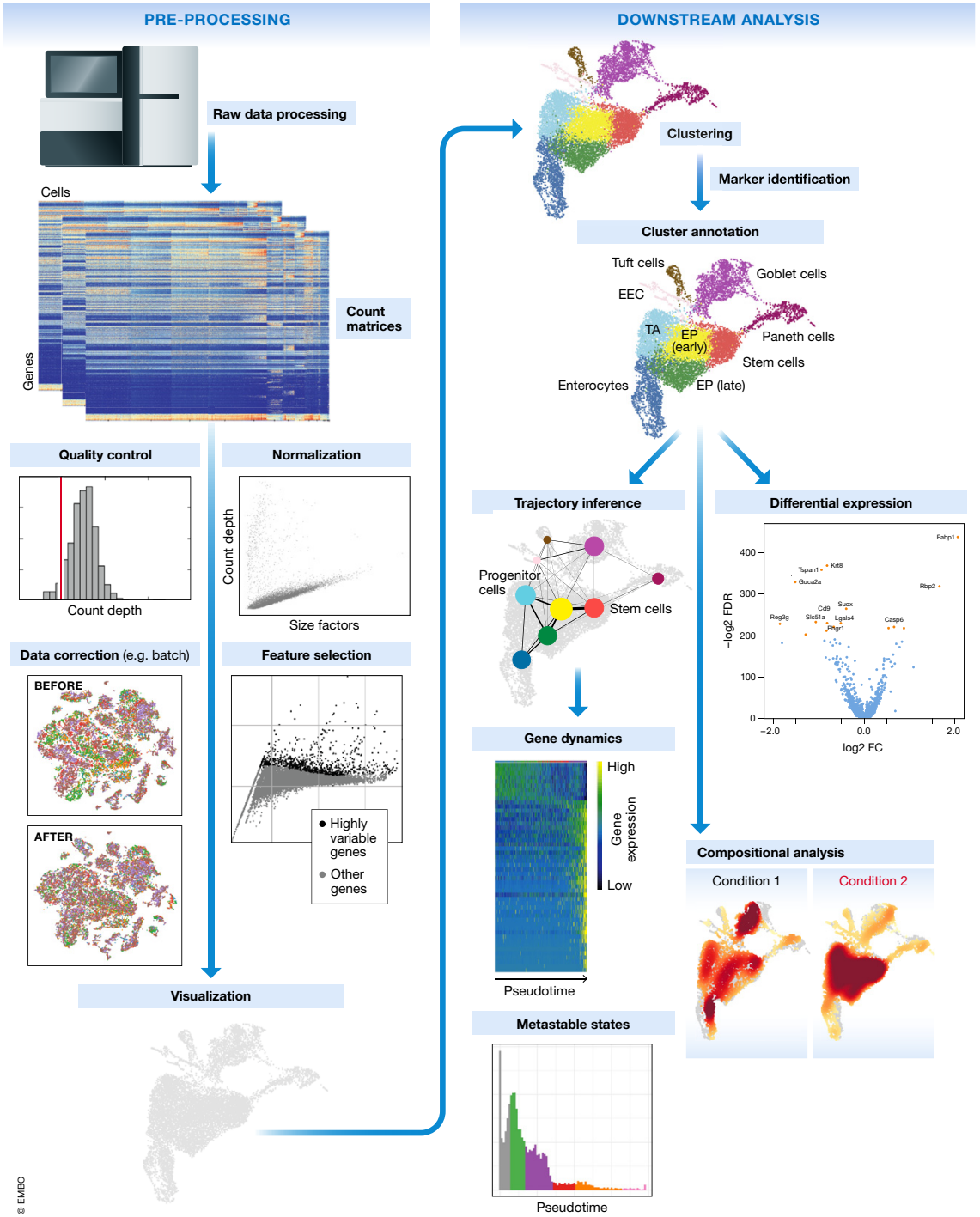

What questions do you have about today's material?

Top

Exercise!

Load, preprocess, and visualize a scRNAseq dataset generated from a time course of embryoid bodies